UNIVERSITÀ DEGLI STUDI DI PADOVA

DIPARTIMENTO DI BIOLOGIA

Corso di Laurea magistrale in Biologia Evoluzionistica

TESI DI LAUREA

Investigating the variance in wing melanization pattern among colour dimorphic males of the wood tiger moth (*Arctia plantaginis*)

Relatore: Prof. Andrea Augusto Pilastro
Dipartimento di Biologia (Università di Padova)

Correlatore: Dott.ssa Melanie N Brien
Faculty of Biological and Environmental Science
(University of Helsinki)

Laureando: Paolo Majorano

ANNO ACCADEMICO 2022/2023

Investigating the variance in wing melanization pattern among colour dimorphic males of the wood tiger moth (*Arctia plantaginis*)

Four A. plantaginis females surrounding two males of two different colour morphs. Photo by Paolo Majorano.

ABSTRACT

In my thesis work the variability in the pattern of wing melanization observable in the males, dichromatic, of the moth *Arctia plantaginis* was analyzed. The species is an interesting case study to test theories on selection of traits thanks to its multiple ecological interactions based on wing coloration: *A. plantaginis* is an aposematic species that presents a male polymorphism in hindwing colouration (yellow or white), maintained by the trade-off of natural and sexual selection.

The sample used comes from a stock population reared for many generations at the University of Jyväskylä (FI). The central aim is to confirm the presence of variability in the deposition of black pigment on the wings and test whether this can be related to the expression of a specific hindwing colour in males. To do this, the wings of 140 males were photographed, with genotype known for the locus of wing coloration. The wing morphometric analysis, of forewing and hindwing separately, was performed in R using Patternize and Recolorize, two packages that allow automatic detection and analysis of colour patterns variability. In second place, the correlation of pattern extension with both hindwing colour and colour locus genotype was evaluated. Finally, I assessed the adequacy of the arbitrarily binary classification (*plus*, *minus*) of the trait "degree of melanization", adopted in the laboratory and based on hindwings.

The analyses allowed to ascertain that the variation in the melanic pattern derives mainly from differences in the abundance of synthesized pigment, to confirm previous hypotheses on the presence of a genetic component, albeit limited, in the variability of the trait, and to detect a slight correlation between hindwing colour and melanization. The melanization categories found support in the distribution of the sample under examination, however, within the category of higher melanization there was a greater variability in melanization that cannot be exploited by this binary subdivision.

CONTENTS

INTRODUCTION

Nature shows us a multitude of shapes and colours, and colour has always been one of the most alluring aspects for evolutionary biologist in history. From Gregory Mendel with peas that come in different colours, to C. Darwin, H.W. Bates, and A.R. Wallace with animal models, and all the others that followed, difference in colour patterns between organisms has always represented something to investigate, to explain.

After Darwin's theory of evolution, animal coloration has represented a superb model system for testing and expanding evolutionary theories, in the attempt of understanding evolution. Colour patterns mediate the interactions between an organism and its environment at any moment of his lifecycle, playing important roles in both intraspecific (e.g., mating and competitive behaviour) and interspecific interactions (e.g., predator-prey, parasite-host interactions), and it also may help the animal maintain its physical state (e.g., thermoregulation, protection from solar radiation and abrasion) (Cuthill et al., 2017).

In many cases particular colorations are employed as visual stimuli to gain benefits form advantageous interactions with another organism (Cuthill et al., 2017) . How this benefit affects the fitness of the individual depends on the type of interaction; predator-prey interaction and mating behaviour are probably two of the most iconic types of interaction based on visual signalling, where the benefits would be, respectively, an increment in survival or reproductive success.

Being potentially exposed to this plethora of selective pressures, makes colour pattern evolution very likely to be shaped by selection for the best coloration. For that reason, the diversity of colours, as well as colour polymorphism, is therefore valuable to understand the processes generating and maintaining biodiversity (i.e., genetic variation) in the wild (Nokelainen et al., 2012).

Signals in Predator-Prey Interactions

Prey survival strategies against predation associated with coloration, can be roughly dividend in 2 great families: camouflage, to avoid detection or recognition as a prey, and aposematism (or warning), to deter, actively eliciting avoidance. Prey camouflage consists in assuming colourations, patterns, and morphological shapes that hinder its recognition as a prey by the predator. That is attained either by blending into the environmental background to avoid detection (crypsis), or generating false impression about its real appearance, with colour contrasts generating false edges inside the prey frame (disruptive camouflage) (Adams et al., 2019). Aposematism is an anti-predator strategy by which the prey advertises its defences against predation with warning signals directed at predators, which often include conspicuous colorations (Rojas et al., 2015; Ruxton et al., 2004). In aposematic organisms a primary defence, operating before the attack (e.g., distinctive colour), is coupled with a second line of defence (chemical, morphological or

behavioural) that makes the prey unprofitable or dangerous for the predator, as it gets bitten (fatally or not).

Since it is beneficial for both sides that the predator learns quickly to avoid the defended prey, natural selection strongly favours conspicuous colorations in the preys, clear and easy to remember and discern after few encounters (Cott, 1940). Aposematic colorations usually make use of vivid colours, such as red, orange, or yellow hues (Rojas et al., 2018); at the same time, colour patterns with high internal contrast (e.g. salamanders' and skunks' black and white, or wasps' yellow and black) are expected to be learned faster (Rojas et al., 2018; Zylinski & Osorio, 2013). Variability can inhibit predator learning by decreasing the frequency of encounters with each warning signal and increasing the number of signals to remember, hence purifying selection is expected to act on colour patterns, toward monomorphism (Hegna et al., 2013; Joron & Mallet, 1998). Polymorphic warning signals in aposematic systems are therefore enigmatic because predator learning should favour the most common form, creating positive frequency-dependent survival. In contrast, polymorphism in aposematic coloration is observed in numerous species (vipers: Martínez-Freiría et al., 2017, frogs*:* Rojas, 2017 and Noonan & Comeault, 2009, newts: Mochida, 2011; Coleoptera: Kozlov et al., 2022 butterflies: Idris, 2013; moths: BRAKEFIELD & LIEBERT, 1985). The unexpected phenotypic diversity observed in aposematic systems is extremely fascinating, because the obvious uniformity advantage in predation avoidance must be traded off for fitness benefits in other contexts (e.g., homeostasis and/or reproduction). When colour polymorphism occurs with several discrete colour phenotypes (polyphenism), those are often associated with differences in morphological,

Figure 1. **Variability of aposematic signals.**
A-F) examples of aposematic colorations from distantly related aposematic organisms (Rojas et al., 2018); G) Different morphs of the aposematic frog *Ranitomeya imitator* (Briolat et al., 2019).

physiological, and behavioural traits (Cuthill et al., 2017). Maintaining polymorphisms within populations requires balance in selection regimes that provide similar fitness benefits across multiple morphs over evolutionary timescale (Maynard Smith 1982; Pryke 2007), so morphs showing a sub-optimal aposematic defence are expected to make up for that by having developed higher functionality in other tasks. As it has been suggested, "*if selection favours specific trait combinations, it can generate genetic correlations representing alternative adaptive peaks*" (Cuthill et al., 2017). Uncovering these different combinations of traits and their fitness effect in each morph is a central topic of evolutionary biology, since the evolution of the trait of interest (i.e., aposematic coloration) has been correlated to the evolution of other traits.

1. Melanization

Melanins are the most common pigmentary determinants of animal coloration (Majerus, 1998). There are two kinds of melanin found in animals: pheomelanin (yellow to red-brownish coloration) and eumelanin (brown to black hues); the latter is the most prominent and studied in insects. Melanin-based coloration has important functions in animals, including a role in camouflage and active signalling, thermoregulation, protection against UV-radiation and pathogens (Fig. 2, Roulin, 2014). One example is the melanization cline of human skin with latitude: the hue gets darker at lower latitude where UV radiation is higher, as adaptation to shield tissues from UV deleterious effects (Jablonski & Chaplin, 2000). Many birds and mammals found in humid and warm environments are more pigmented than populations found in colder and drier areas, even when compared to conspecifics (Gloger's rule). More melanized fur and feathers are thought to be an adaptation that grants higher protection from microbial communities that are more favoured in warm and wet conditions. Yet, what could be true for homeotherm organisms could be unlikely for ectotherms, for which melanization is a key feature in heat absorption, which is necessary to actively move in cold environment (Clusella-Trullas et al., 2008; Hegna et al., 2013).
The different physiological needs and the relevance of melanization among organisms set the base for taxa-specific and species-specific trade-offs in melanin trait expression in different environmental conditions.

Melanin in insects has a prominent role in regulating many physiological processes that potentially make the regulation of its synthesis more crucial for them than for vertebrates. For example, this pigment, aside from body colour patterning, is one of the three major synthetized pigments deposited in developing wing scales of butterflies and moths, with ommochromes and pterins (Kuwalekar et al., 2020; Wittkopp et al., 2009). Adults' pigments start appearing on body and wings during late pupal stages.
Melanin pathway and its components, given the wide range of physiological processes in which is involved, are conserved across insects. Melanin and related

pigments such as DOPA-melanin, dopamine-melanin, NBAD sclerotin, and NADA sclerotin, contribute respectively to the production of black, brown, yellow, and white (colourless) coloration in Lepidoptera and many insects (Kuwalekar et al., 2020).

Melanin molecule in insects and other arthropods also plays a central role immune defence to resist pathogens in the encapsulation response: organismal intrusions elicit rapid synthesis of melanin to encapsulate the foreign body (Sugumaran, 2002). This non-specific immune defence is opposite to the specific adaptive immunity by immunoglobulin response functioning in all jawed vertebrates (Das et al., 2012). Furthermore, ectotherms rely on solar radiation to warm up and black colouration grants higher heat absorption and better thermoregulation in colder environments, increasing fitness (Clusella-Trullas et al., 2008).

In accordance with the thermal melanism hypothesis (darker individuals are advantaged in cool climate), there is documentation on several butterflies that present more melanized forms at higher altitude and latitude. Thermoregulation benefits derived from increased melanization can also grant better escape ability, increasing predation aversion, from faster warm up and take off, and enhanced flying capability (Kingsolver, 1987). Escaping faster from predators and increasing flight duration, thanks to a more efficient thermoregulation, give melanized individuals more time to find food, suitable mates and suitable oviposition sites (Lindstedt et al., 2020).

Melanin-based black pigment is costly (Lindstedt et al., 2016), and while being part of animal coloration and warning signals, it is expected to trade off with other fitness-related traits. For example, darker individuals have been shown to face

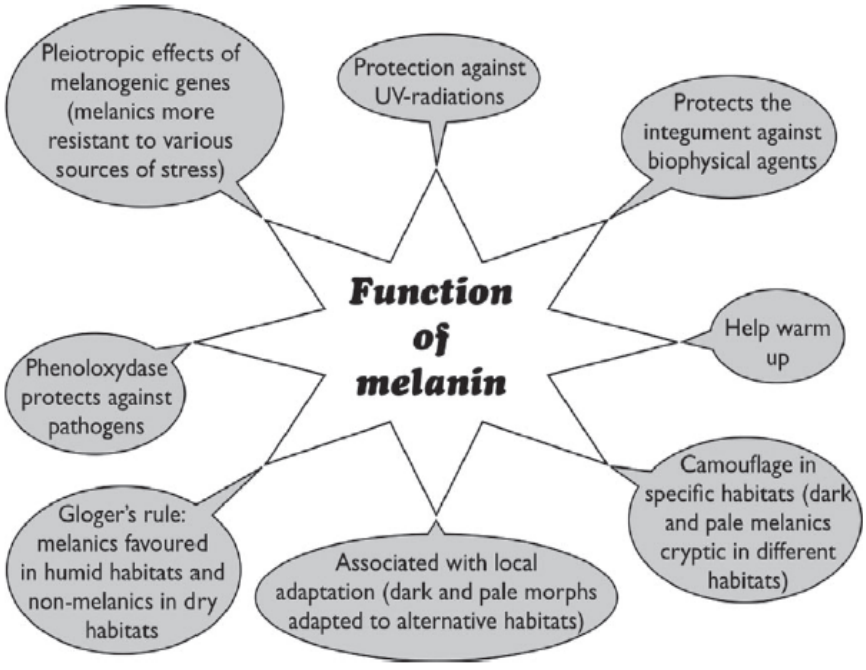

Figure 2. **Adaptive functions of melanin-based colouration.** (Roulin, 2014)

slower development, especially when facing stressful condition (Talloen et al., 2004), possibly because melanin synthesis require nitrogen, limited resource for herbivores as Lepidopteran and many other insects (Lindstedt et al., 2016; Ojala et al., 2007; Talloen et al., 2004).

When melanin-based colour pattern also possesses warning or signalling functions, benefits and costs of melanic colouration can be harder to evaluate. Melanin production in these cases can influence the defensive strategy and its fitness consequences also depend on warning signals evolution at the individual and population levels, depending on the colour pattern of the conspecifics and the associated complex frequency-dependent selection dynamics (Doktorovová et al., 2019; Hegna et al., 2013; Kozlov et al., 2022; Lindstedt et al., 2020; Speed & Ruxton, 2007). An iconic evidence of that was found in the alpine population of the aposematic wood tiger moth (*A. plantaginis*), in which an increment of melanized area improves thermoregulation but hides the bright warning colouration, to the point that determines higher predation (Hegna et al., 2013). Evidence of an aposematic cost in more melanized individuals were found also in some Finnish wasp populations (Badejo et al., 2018).
When aposematic signals are based on contrasts between black pattern and bright colours, intra-population polyphenism in melanic coverage can stem from trade-offs that gives equal fitness to different morphs and be maintained under various balancing selective forces. The polyphenism maintenance can also occur thanks to different predator response to the black pattern contrast, each presenting a different optimum in prey's melanic coverage (Doktorovová et al., 2019) or high environmental heterogeneity and variability, with different morphs advantaged in different conditions (Fig. 3, Kozlov et al., 2022).

Figure 3. **Color morphs of *Chrysomela lapponica.***
Left to right: orange, light patterned, dark patterned, black (Kozlov et al., 2022).

All this plethora of processes in which melanin is involved in determines the intrinsic complexity of investigating evolution and maintenance of polymorphism in melanin phenotypes, that often involve several trade-offs with other fitness-related traits expression.
To further increase complexity of melanization pattern evolutionary studies, many holometabolous insects changes drastically their appearance and ecological interactions during their lifecycle. Coloration in this case have different functions and melanin pigments can be involved in shifts of trade-offs optima between one

function and the other, based on stage-specific needs. Stage-specific selective pressures can drive the evolution of melanization trait in opposite directions, such as favouring a phenotype in larval stage (e.g., thermoregulation or predator avoidance) and then selecting another genotype for adults (e.g., for reproductive success) (Lindstedt et al., 2016).

2. Study species – *Arctia plantaginis*

2.1 Distribution and Life Cycle

Arctia plantaginis, the wood tiger moth, is an aposematic arctiid species with a wide distribution in the Holarctic region (Hegna et al. 2015).

In most of Europe, males of *A. plantaginis* present either yellow or white hindwings that serve as a warning signal and show variable black patterning. Female hindwing's colour is also variable but shows a continuous variation from yellow to red; females present more melanic hindwings than males, and less variation for that trait (Fig. 4). Forewing black and white colour pattern, in contrast, does not show significant variance between sexes, nor within and among populations in northern Europe. Hereafter, I will use the term "colour" referring to the yellow or white hindwing background colour of males and refer to the extension of the black pattern on the wings as "melanization".

In Finland the life cycle of the species in the wild is characterized by one generation per year (univoltine species). Females lay eggs (200 on average) on vegetation in late summer, during the short mating season, and have been found on different plant species, hence there are no evidence for preference toward a specific host plant. The larvae hatch approximately after a week; caterpillars are polyphagous (generalists, feed on different plant species), and grow until winter, before entering in a diapause state to overwinter under the snow. In spring, caterpillars resume feeding until pupation. Metamorphosis into adults occurs after a week or more.

Adults of this species are capital breeders, that means they do not feed, but rely on previously accumulated reserves to reproduce. Adults die after reproduction (performing one or more matings), determining that complete allocation of resources accumulated during the larval stage into reproduction.

Females are sedentary, and usually only males disperse and fly around at daytime in search of female for reproduction; thus, only males are responsible for the gene flow between nearby populations.

The reproduction takes place at dusk when females climb to elevated spots (e.g. tree trunks) and start their "pheromone calling" to attract males also from long distances through the release of volatile chemicals (pheromones) that are intercepted by males' feathered antennae (Pasqual et al., 2022).

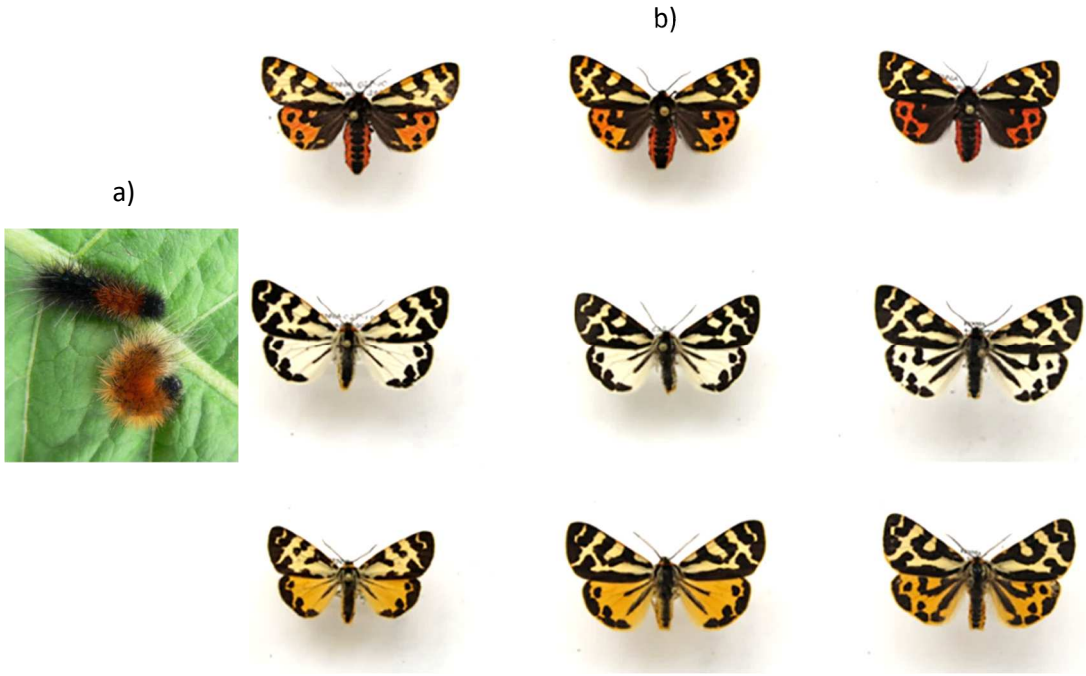

Figure 4. **Variability of *A. plantaginis* from stock population.** a) Two *A. plantaginis* caterpillars with variable signal size (Lindstedt et al., 2020). b) Adult phenotypes of females (first row), white males (second row), and yellow males (third row); different levels of melanization are shown: *plus* males are in the third column. (Briolat et al., 2019)

2.2 Anti-predator strategies based on visual signalling

A. plantaginis is aposematic across all its life stages because its warning coloration (primary defence) represents an honest signal of the disgusting taste that makes them an unprofitable prey (secondary defence). Caterpillars show a large orange spot on black background (Fig. 4). Adults advertise avian predators of their chemical defence with their brightly coloured, highly contrasted wings.

This species has attracted the attention of many researchers over the years, thanks to its colour polymorphism that contrasts with the expectations for aposematic organisms and allows exploration of multiple selection scenarios, while applying and testing for evolutionary theories. Despite the drastic variability in wing colours shown, all morphs have been proven to be conspicuous to the predator on green foliage, their natural resting position in the wild ((Honma et al., 2015), Nokelainen et al. 2012), as during flight (Henze et al., 2018).

Although not investigated yet, this moth could also be relying on a deimatic strategy, employed by many other moths, especially by *Catocala spp*, called underwing moths (Schlenoff, 1985). Deimatic behaviour is based on the sudden exposure of a previously hidden conspicuous visual colouration to predators at close distance, that can trigger an unlearned avoidance response in predator causing it to slow or stop its attack (Drinkwater et al., 2022; Holmes et al., 2018). The aforementioned strategy in moths consists in a sudden disclosure of the forewings, with the display of the conspicuously coloured hindwing, previously hidden under the forewing. Since the wood tiger moth spend much time basking,

so that their conspicuous hindwings are covered by forewings until they decide to take-off, when disturbed, that behavioural strategy could be part of this moth's anti-predator strategy. Deimatic behaviour and aposematism require equally conspicuous coloration of some body part, so that aposematic coloration can be employed in deimatic display and the traits can coevolve to a certain extent (Drinkwater et al., 2022). Nevertheless, deimatic behaviour is primarily aimed at catching the predators off-guard and not to advertise unpalatability, differentiating it from the aposematic "strategy", and that could generate different selective pressures. For example, rarer colours could generate more shock since the predator is not expecting that.

Interestingly, in this species the bright colour contrast is not the only features of the wing pattern that can confer protection against avian predators. Honma et al. (2018) provided experimental evidence for a dual function for the forewing colour pattern, where the bright coloration (signalling) has been tested to have an efficient disruptive marginal pattern (camouflage). The key point in the evolution of this paradoxical double-function in *A. plantaginis* is that the wing patterning has evolved to have different detectability on different backgrounds, such that "*the moth is conspicuous when it rests on vegetation, but when it feigns death and drops to the grass- and litter-covered ground, it is hard to detect. This death-feigning behaviour, therefore, immediately switches the function of its coloration from signalling to camouflage*" (Homma et al. 2018). The evolution of this second function of the wing pattern can reduce the cost of higher detection risk, by predators that decide to ignore the warning message (either because of naiveness or toleration to chemicals).
While death-feigning behaviour has been shown to be employed more frequently by females (Honma et al., 2015), the deimatic strategy could give more advantages to males, which are more likely to escape by actively flying, although the two strategies could potentially be used alternatively. It is fascinating to observe how much the hindwing's pattern of less melanized males come to resemble the one of *Catocala spp*, with just one melanized band marking the distal edge. On contrary, females have more melanized hindwings and lower colour contrast. Taken together with their less agile flight, this suggests that the deimatic strategy in this sex is presumably less proficient than falling behaviour.

All these observations suggest that aposematism, camouflage and deimatic strategy may have jointly influenced the evolution of colour pattern, possibly with different costs and benefits for the two sexes and for male colour morphs.

Male polymorphic hindwing colouration (white or yellow) follows simple mendelian inheritance. Recently unveiled genetic basis (Nokelainen et al., 2022) consists in a single diallelic locus determining the two male phenotypes, with the "white" allele (W) strictly dominant to the "yellow" one (y). Females can carry and

Figure 5. Male's colour genotypes under visible radiation (Nokelainen et al., 2022). White genotypes WW and Wy are indistinguishable.

transmit both alleles, but do not show any phenotypic cue. Males of both genotypes WW and Wy are white and indistinguishable to human eye (Fig. 5); this observation led to describe the W allele as strictly dominant. However, it was recently discovered that the two white morphs can be easily told apart by both conspecifics (moths and other insects) and predators (birds). In fact, the two morphs' hindwings show differences in reflectance in the near UV range of the light spectrum; these differences are out of human eye perception but conspicuous to birds and insects whose visual system can process those shorter wavelengths (Nokelainen et al., 2022).

Over the last two decades, great effort was spent to uncover the dynamics behind the maintenance of variability in male hindwing colouration, exploring the potential eco-evolutionary mechanisms that prevent one allele from reaching fixation. At the present moment much evidence has piled up on how a wide spectrum of selective pressures, in action on both sexes, could interact to maintain polymorphism at the colour locus. For example, yellow males appear better defended against predators than white ones, relying on a better primary defence, such as better warning colouration (Hegna et al., 2013) and repulsive odour (Rojas et al., 2018), to avoid being attacked. On the other hand the male yellow coloration brings trade-offs in reproductive success (in Finnish population), with lower mating probability (Nokelainen et al., 2012) and reproductive output (De Pasqual et al., 2022), as well as in dispersion ability, since they are less active than white males (Gordon et al., 2015).

Heterozygote advantage at colour locus has also been proven to play an important role in females, where heterozygous individuals (Wy) have higher reproductive success than the other two homozygous genotypes, with benefits in several stages of reproduction (De Pasqual et al., 2022). These female heterozygous advantages can also contribute to the maintenance of male hindwing colour variability.

Another aspect of ecological interactions in this aposematic moth is that predator pressure exerted by local predators changes geographically, favouring different morphs. Unexpectedly, sexual selection has been proven to be positively frequency-dependent, selecting for monomorphism (Gordon et al., 2015). Consequently, assuming gene flow happening between sub-populations with different morph frequencies, a geographical mosaic of selective pressure can have a key role in maintaining this male hindwing colour polymorphism, interacting with other local dynamics (Gordon et al., 2015; Rönkä et al., 2020).

In summary, a trade-off between natural and sexual selection through geographically heterogeneous morph- and sex-specific predation and reproductive success, contributes to the maintenance of this polymorphism (De Pasqual et al., 2022; Gordon et al., 2015; Nokelainen et al., 2012; Rönkä et al., 2020). The previously undetected difference in colouration between the two white morphs adds even more complexity to the landscape of selective pressure that can, therefore, be exerted on males in a genotype-specific way. Few studies have been performed accounting for male colour genotype until now, and expanding the research on this aspect could therefore be of great value for the understanding of this polymorphism maintenance.

2.3 Wing melanization

As previously introduced, there is another component of the wing pattern that varies within and among populations: the degree of melanization. Male hindwings are variable in the amount of black on the wings across all of its geographical range: the black melanin-based pattern usually covers 20 to 70 per cent of the hindwing area (Fig. 4b), with exception of alpine high-altitude populations, with more than 90% coverage (Hegna et al., 2013). Forewing melanization in Europe varies from 50 to 80 per cent of coverage (Hegna et al., 2013).

Melanization variability in this moth is a fascinating and complex field of study, as pigment synthesis can potentially affect warning signalling efficiency in different life stages, sexes and colour morphs while, and at the same time, being constrained by its role as key molecule in a multitude of physiological processes, from UV shielding to immunity response (Galarza et al., 2019, 2021; Lindstedt et al., 2020; Nokelainen et al., 2022). An interesting aspect of this moth pattern expression is that melanization seems to have different signalling functions between hindwings (covering warning pattern (Hegna et al., 2013)) and forewings (contrast and disruptive pattern (Hegna & Mappes, 2014; Honma et al., 2015)), that could favour, locally, the evolution of even more complex regulation of its synthesis.

The melanic black pigment in this aposematic moth is eumelanin derived from dopamine. The white and yellow pigments are also synthesized from dopamine, in a parallel independent pathway. Synthesis of black pigment is expected to be costly, since precursors are scarce in the herbivorous diet (Lindstedt et al., 2016). Both the hindwing coloration and the amount of melanization are heritable (Lindstedt et al. 2009; Nokelainen et al. 2013), with the latter being controlled by a more complex model of inheritance and a greater non-additive genetic variance component.

Generally, in this moth, higher melanization in larvae is maintained in the adult stage, resulting in higher wing melanization (Hegna et al., 2013). Although significant offspring variability in wing melanization exists, it does not seem to be influenced by plasticity, which was found to be non-significant in response to multiple environmental factors, such as temperature, diet, and larvae density. So,

although plasticity in larvae and adult bodies melanization was recently observed in response to different rearing temperatures, these environmental factors did affect adult wing melanization (Galarza et al., 2019). More recently, a resource-allocation trade-off was found at adult stage with respect to chemical defence, as suggested by a negative correlation between degree of black coverage and chemical defences when resources are abundant (Ottocento et al., 2022). In a similar way, when resources are scarce, males with higher hindwing melanism develop smaller hindwings and forewings, evidencing how melanization could set a limit to resource allocation for tissue growth (Ottocento et al., 2022). It is plausible that the trade-off between physiological and signalling function of melanin reached different equilibria in *A. plantaginis* populations inhabiting diverse environments. One example of that has been found by Hegna et al. (2014), who found that allopatric Alaskan populations express locally different forewing black pattern, depending on the granularity of the background that influence the effective disruptiveness of the pattern.

After depicting the broad spectrum of selective pressure tested until now, on both colouration and melanization, I think that there could be some value in starting to consider also deimatic behaviour as a factor for polymorphism maintenance. Since deimatism is based on taking predator by surprise, the rarer the signal, the bigger is expected to be the startling effect; likewise, the most conspicuous is the visual signal, the stronger the predator response. Applied to the system of study, we can make the following predictions: 1) a potential benefit could come from exposing less frequent coloration when performing the behaviour, and 2) with lower hindwing melanization, the signal exposed would be more conspicuous (Hegna et al., 2013). This strategy is therefore expected to be negatively frequency-dependent and to favour a lower degree of melanization.

2.4 Arctiid's wing melanisation pattern

It is known that Arctiid moths show an large variability in patterning both within and across species (Fig. 6, from Gawne & Nijhout, 2020). Across *A. Plantaginis* geographical range, the observed variability between population could be due to different mechanisms, such as changes in size, shape, and/or positioning of the principal pattern elements. The intraspecific pattern variation can be due, for instance, to difference in size of the elements, determined by the amount of melanin stemming from the deposition sites: black patches could expand, varying the pattern profile by eventually extinguishing some of the light-coloured patches. Although pattern elements can change in shape on parallel with size changes, developmental changes in pattern element shape may occur by different disposition of secretory cells, producing shape differences independent from melanin quantity (Gawne & Nijhout, 2020).
Little work has been done on wing pattern diversity of wood tiger moth in Europe, so the nature of this variation is still unexplored. In Alaska, forewing pattern

variance was studied on close-by allopatric populations possessing a greater range of variation than in Finland (Hegna & Mappes, 2014). From previous studies, not focused on colour pattern, it appears that European populations show lower variation (Galarza et al., 2014).

What has not been investigated yet is the variation in hindwing melanization, that is not likely to interest the ecology of moth at resting position, but comes into play during take-off and flight, when it is exposed to predators and conspecifics. In addition to that, the intra-population variation in wing melanization pattern between the two white genotypes, has yet to be tested: the interest about melanization concerns both its potential significance as correlated trait in evolution of polymorphism (e.g., heterozygotes advantage) and its applicability as valuable discriminator between the two cryptic white genotypes.

Melanin is a key physiological factor, and increasing the knowledge on the nature of its variability in this species is important to understand if it is possibly shaped by selection and also to deepen the understanding of visual signalling dynamics of *A. plantaginis*. The interest in variability of melanic pigmentation in animals is transversal to this case study and Lepidoptera in general. Investigation on this moth can bring insight on the evolution of this molecule's production towards a wider understanding of how the expression of a trait under multiple selective pressure (melanin production) is shaped by unavoidable trade-off.

3. Wing Pattern Analysis in Lepidoptera

Colour patterns can be easy to observe and describe, but their quantification and rigorous comparison is challenging. Moreover, the wing pattern as we (human) see it in the lab could be perceived way differently in the wild, light conditions can be sub-optimal in many cases and other animals' visual system could have developed specific adaptations (Nokelainen et al., 2022).

3.1 Wing pattern models

Pattern in lepidoptera wings is generated during the pupal stage, colour patches stem from the deposition of morphogen and then actual pigment from specific point sources on the wings, mainly from the veins. Pattern variability can be generated by changing the position of morphogens' deposition sites, changing the amount of pigment synthetised or alternative switch-on of some of them.
Butterflies' and moths' wing pattern can be decomposed in the underlying system of homologous elements within and across many species, allowing intra- and inter-species rigorous comparisons, allowing to precisely describe the outcome of experiment on pattern development mutation (Mazo-Vargas et al., 2017), and also identify trends in pattern evolution (Monteiro, 2008). The system is based on the notion that venous junction points on the wing provide positional information

which essentially anchor the primary characters to one region of the wing, rather than another, allowing to define homology in elements positioning even between distantly related individuals (Gawne & Nijhout, 2020). For this aim, two theoretical archetypes were designed, the first and historical one is the Nymphalid Ground Plan, "NGP" (Nijhout, 1991), that perfectly matches all Rhopalocera wing patterns, and recently the "arctiid archetype" was proposed to be the analogous for moth's forewing.

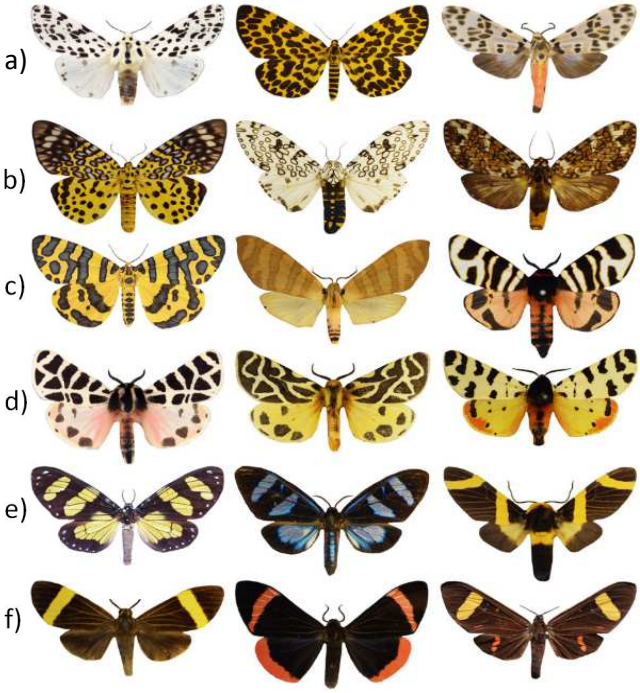

Figure 6. Pattern models based on the Arctiid Archetype. (Gawne & Nijhout, 2020)
Wing pattern variability in Arctiinae subfamily:
a-b) Two types of spotted pattern. c-d) Two types of banded pattern. e-f) Two types of bold pattern.

The arctiid moths exhibit some of the most pronounced intraspecific forewing pattern variation found in the Lepidoptera, mostly presenting a black melanic pattern on a coloured background (Gawne & Nijhout, 2020) that can be classified in three broad phenotypic classes: spotted, banded, and bold (Fig. 6). A spotted pattern is defined when, the intervenous elements composing the fundamental pattern elements, take the form of a highly discretized series of spots arranged in columns perpendicular to proximal-distant axis (Fig. 6a-b). In banded phenotypes the pattern elements are solid stripes that run antero-posterior across the wing, with more or less regular interruptions by horizontal patches of background colour (Fig. 6c-d). Bold phenotypes are characterized by the presence of contiguous melanic regions, result from the fusion of characters, that are interspersed with smaller islands of background coloration (Fig. 6e-f) (Nijhout, 1991; NIJHOUT & WRAY, 1988).

3.2 Pattern sampling

The process of pattern analysis generally follows 3 phases: 1) Pattern extraction: pixel clustering by colour that allows distinction of the pattern elements from the background colours; 2) Variance analysis: statistical evaluation of the variability in shape, colour contrast, and other features, depending on the type of information extracted in the first step; 3) Assessing the biological significance of the variance: frame the variation founded in a biologically relevant way to answer specific questions on the study system (e.g., evolution of divergent signalling, or divergent developmental pathways, inter- or intra-specific individual discrimination). For the

first two steps, the mechanical pattern analysis, a suite of different tools can be used; whereas the approach to the third step depends on the biological question and organism studied.
Here is an example of the four most commonly used tools for colour pattern geometry investigation: Endler's adjacency and boundary strength metrics (Endler, 2012; Endler et al., 2018), focusing on contrast between adjacent colour patches that define salience of the pattern; *patterize* R package (Belleghem et al., 2019), which quantifies pattern variation essentially based on a sampling grid; the *micaToolbox* suite of tools for multispectral image analysis in ImageJ (van den Berg et al., 2020); and the matching of spatial image data with spectral reflectance data in the *pavo* package (Maia et al., 2019).
The choice between one method over others only depends on the question of the study, some of them can measure variation in different visual systems, extending the analysis to UV radiation reflectance (*micaToolbox* and *pavo* R), others, like Patternize, can grant a more intuitive and customizable framework in comparing human-visible variation in colour patterns, especially when a black pattern or background is interested (Van Belleghem et al., 2020; Yuan et al., 2022).

In general, the workflows of quantitative pattern variance analysis are based on a first step of generation a "colour map", where the image is discretized in different patches of uniform colour, and a subsequent measure of patches variation across the sample. The measure of variation refers to how various aspects of these patches (e.g., shape and hue) vary across images and can entails representation in a PCA environment, dendrograms of colour hue similarity and other statistical tools to describe the variation (Weller et al., 2022).
The intrinsic difficulty in reliably generating the colour map is at the base of the development of Recolorize*,* an R package made to solve some of the issues in colour clustering and colour map generation that can be encountered in the first step of other methods. The general process is: 1. initial clustering step; 2. refinement step; 3. optional semi-manual edits; 4. export to desired format (Weller et al., 2022).

Recolorize was made to work synergically to other tools. The main function of this package is to generate colour maps (colour clustering step) in the most efficient and reproducible way, to be exported and analysed through each of the four aforementioned pattern analysis suites. Patternize is a package that provide a toolbox of functions and an essential workflow to assess variation in shape and extension of colour patterns, netted from individual structural variation in dimension by alignment to homologous landmarks. The target colour is extracted, and the colour map is a binary matrix for presence (1) and absence (0) of the pattern in each unit of area. On this pattern matrix it is performed a PCA, which allows visualizing the main variations in colour pattern boundaries among or between groups of samples. Furthermore, it can show the predicted colour pattern changes

along the principal component (PC) axis. Prediction on colour pattern presence is based on proportion of samples showing pattern in a specific unit of area; positive values indicate presence, negative absence. In addition to that it also returns a quantification of pattern area.

The data obtained from these suites of analysis, can be directly use as discriminants in matters of taxonomy, development, and broader investigation on pattern evolution dynamics. First of all, pattern coverage quantification per se is a requirement to approach the genetic study of a pattern expression in a quantitative framework (i.e., QTL mapping). Where phenotypic variation is continuous or difficult to assess any categorization carries represent a limitation to a certain extent. Furthermore, the reliable and reproducible analyses of pattern shapes variation give us a great asset of data to address the study from an evo-devo point of view, reasoning on what kind of variation are we observing in the species of study, be it a change pattern ground plan or just variation in proportion of pigments synthetized.

4. Aims of the study

The idea underlying my work is to explore the possibility that some elusive variation in black pattern shape and/or coverage can determine different benefits that contribute to the maintenance of polymorphism in aposematic coloration. My broad aim is to shed more light on the melanization phenotype in this species, assessing whether it is a factor capable of influencing evolutionary dynamics of its polymorphism in aposematic coloration.

It is clear from the start that the sample size in this experiment is quite limited in terms of number of families used, that is why the study aims at the discovery of macro differences and trends in wing melanization pattern, and collect valuable information about the aspects to further investigate.

First of all, I wanted to ascertain the nature of the wing melanization pattern variability in of male *A. plantaginis* observed in its Central-Southern Finland populations. The two opposing hypothetical scenarios for variation in pattern shape are the following:

1) A continuous gradient in the amount of pigment synthetized at wing level determines the general enlargement or contraction of the pattern shapes boundaries, reflecting melanin expression levels.
2) Rearrangement of pattern elements disposition and shape (change in morphogen deposition sites) can generate different melanic patterns, independently from quantity of black pigment deposed.

My second object is the investigation of potential correlation between hindwing colour expression and wing melanic pattern shape and coverage (in forewings and hindwings), with an eye to the maintenance of colour polymorphism.

Another point of my work concerned the visual discrimination between white genotypes: my intent was to search for possible morphological discriminants between the two genotypes in wing melanization pattern, both in hindwing and forewing. Due to genotyping requirements, such as detachment of body parts with a consequential fitness alteration, an external discriminator would be extremely beneficial in handling living white males of unknown pedigree (e.g., wild caught), used in most of the behavioural experiments carried out in the laboratory.

A side aim of this work is to assess the adequacy of a binary classification of male melanization phenotype based on hindwing pattern, that is generally used in the phenotyping of Finnish and Estonian individuals in our lab, to compile the pedigree data frame: *plus* or *minus*, respectively with more or less melanized hindwings (See Materials and Methods for the criteria). Is it matching a real bimodal distribution in hindwing melanization? If so, it also a good proxy of overall wing melanic coverage? Is there space for other phenotypic classes to enhance the categorical definition of the melanin phenotypes?

In my investigation I will use two R packages for pattern variability quantification never used before on this species and it is my intention to test their functionality in wing pattern area quantification, with the intention of optimizing a semi-automatic workflow for pattern quantification. There are two reasons for which a rapid and repeatable pattern quantification would be extremely important: 1) Generation of larger datasets to perform QTL mapping and uncover genetic bases of wing melanization (e.g., Bainbridge et al., 2020), still impossible with the less automated method used until now (i.e., pattern area calculation in ImageJ, Ottocento et al., 2022); 2) Rapid phenotyping of wild individuals to quantitatively assess the temporal variation of melanin phenotype in the wild, to record its more subtle variation. Moreover, the monitoring of phenotypes involved in thermoregulation could represent a great asset to track climate change effects, as reported for other organisms (Karell et al., 2011).

My study ultimately aims at obtaining an accurate measure of melanization phenotype – the black pattern on the wings – to analyse its correlation to colour morphs and genotypes. Working on quantitative evaluation and efficient intra-specific comparison of the phenotype was a decisive step toward a more effective evaluation of intraspecific variability and the individuation of genetic bases of the trait's variation. To answer these questions, I analysed the Finnish laboratory stock of *A. plantaginis*, using the R packages Recolorize and Patternize to obtain a map of colour pattern variation and melanic colour coverage.

MATERIALS AND METHODS

1. Moths Rearing and Sample Collection

The individuals analysed in this work were part of a laboratory stock originating from Finnish wild caught individuals that has been reared at the University of Jyväskylä since year 2013, under laboratory conditions (hereafter referred to as "stock population").

In laboratory conditions, it is possible to rear up to 3 generations per year, with the last destined to overwinter as larvae (in the fridge, -4°C). The rearing takes place in a greenhouse, at controlled density (maximum 20 larvae per container) and temperature, around 23°C in the day and a night temperature of at least 16°C. To perpetuate the stock mating pairs are carefully chosen from the known pedigree, to avoid inbreeding, that could affect the moths' survival and the experimental results and preserve the genetic variability. Moreover, the laboratory population was complemented yearly with wild individuals collected from the same populations that founded the laboratory population.

Three genotype lines (WW, Wy, yy) have been established in the laboratory stock for experimental purposes and are maintained through controlled mating to maintaining as much genetic variability as possible. The mating is performed in humidified plastic boxes (13H x 7W x 9L cm) with a mesh cover to allow ventilation. After fecundation females lay on average 250 eggs (Chargé et al., 2016), and approximately 7 days later caterpillars hatch and start eating fresh leaves. The larvae experience natural light conditions, while fed daily, *ad libitum*, with fresh dandelion (*Taraxacum spp*) leaves, or alternatively salad (from March to late of May), when wild dandelion is not available. After 14 days the caterpillars are divided, 20 each box, until pupation. Pupae are removed daily to avoid cannibalization by other larvae, stored singularly in pots and humidified by means of a wet a sponge until eclosion. Adults do not feed and are used for mating, selection assays, or directly frozen for further analysis. All individuals of the pedigree are stored at -20°C. The life-history traits (e.g., fecundity, hatching success, offspring survival, and mating success) are recorded afterward.

After eclosion, adults are given an identification number that shows their lineage (FI, "Finnish", EST = "Estonian"), the year they have been reared in (i.e., "21" stands for 2021), the generation number (from 1 to 3), the family number and the sequential individual number. In example: FI21.2-35.4 refers to the 4° individual of the 35° family in the 2° generation reared in the year 2021. At the same time moths are sexed and pigmentation features are registered. Adult's pigmentation features are assessed by eye, refer only to hindwing appearance: 1) Males' hindwing colour – white (genotypes; WW, Wy) or yellow (genotype; yy); 2) Hindwing melanization – plus (+, more melanized) or minus (-, less melanized).

The main discriminant in melanization assessment is the thickness of the two lines that occupy the central part of the wing (Fig. 7):

1. *Plus* phenotype shows bold stripes, where the upper one assumes a solid hook shape (Fig. 7b); in some case black scales can expand further above the hook (Fig. 7a)
2. *Minus* phenotype ranges from 2 tiny and short black stripes, in the proximal part of the wing, to no black line at all (Fig. 7c).

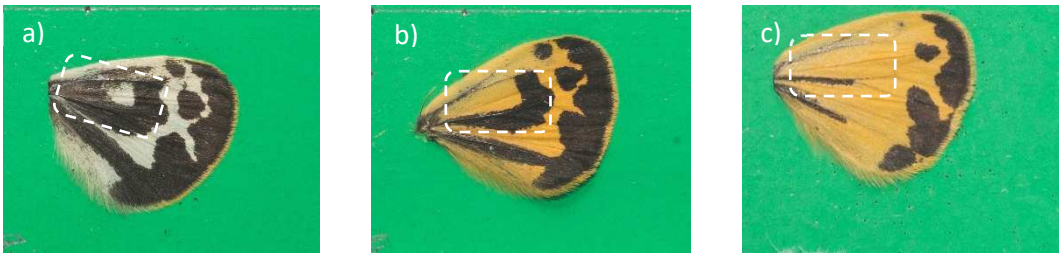

PLUS (W_) **PLUS (yy)** **MINUS (yy)**

Figure 7. Melanization phenotype assessment. White sectors outline the discriminant areas.

The 140 individuals used in this study are males from 12 genotype lines families (at the colour locus) of the second generation reared in 2021 at Jyväskylä University's facilities; all families are from of the Finnish line. There is an equal number of four families of each genotype, so 10 specimens from each family were sampled, 40 specimens per genotype in total. A total of 120 suitable forewings and 120 suitable hindwings were arbitrarily chosen from either the right or left side based on integrity. Assuming that a potential intra-individual difference in pigmentation is non-significant compared to inter-individual variability. The total number of individuals photographed is higher than the number of wings in each category because not from all individuals was possible to retrieve both wing types.

The wing destined to image analysis are cut off and directly packed into individual paper bags with their ID. Most of the hindwings needed to be spread before the photographing, to allow the extraction of the whole pattern. The wings have been put into wet chamber to regain flexibility, those were isolated containers with paper sheets soaked in water on the bottom (addition of some drops of ethanol help avoid moulting), in which packed wings are deposited and left to loosen up. After 1-2 days wings are prepared with pins and stripes of oven paper, cheaper analogous of entomological paper that do not take the scales off.

2. Photography

Wing photography was carried out with a mounted Samsung NX1000 digital camera with a Nikon EL 80 mm lens. The main lens was attached to two elongation tubes (17 and 25 mm) and via an adapter to the camera body. Camera settings were the following: “aperture priority” (A) mode, aperture of f/11, ISO of 100, Matrix Metering for exposure. High fraction of aperture was required to keep all the wing at focus, the overall exposure was kept constant at an arbitrary value that would allow the best vein recognition (required for landmarking, see below).

The photos were taken in the human-visible range, using an UV and IR blocking filter on the lens, which passes wavelengths only between 400 and 680 nm (Baader UV/IR Cut Filter). A standard light source 75W Exo- terra Sunray (mimicking sunlight across the spectrum) was used. This setting made the image also suitable for spectral analysis of colour, that could be done in future, although none of them were carried out in this study. All images were taken at the same distance and angle from the wings, to avoid distortion. Two pictures per individual were taken on a green background, ventral and dorsal side of the four wings. Each image also included a ruler, the individual ID, a label for “dorsal” or “ventral” side, an Avian Technology Colour Checker to standardize the colour of the images (Fig. 8a). RAW format images were standardized using the automatic white balance extraction on the checker in Adobe Ps 2019 (Camera Raw version 14.3). Afterwards only dorsal side was processed (Fig. 8a), ventral was used as better reference in landmarks positioning.

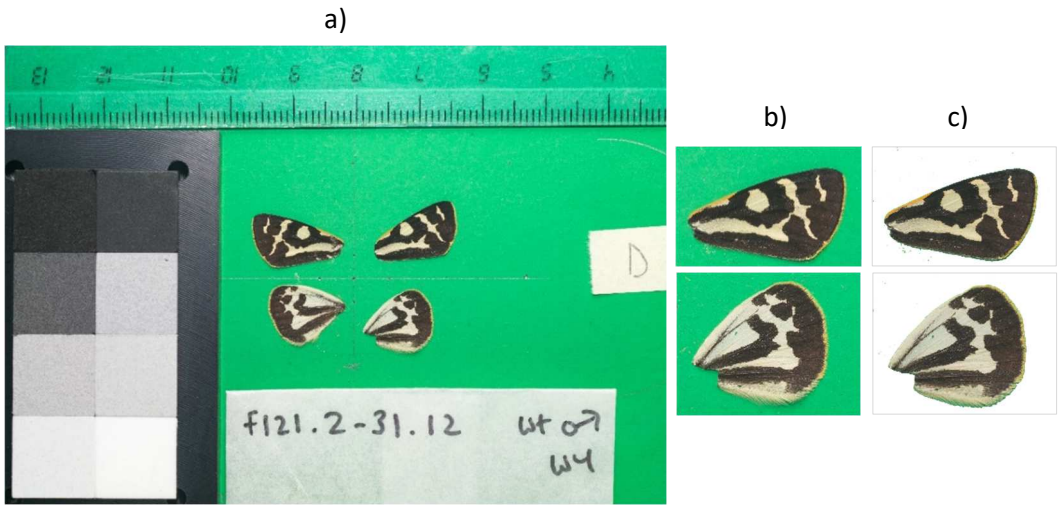

Figure 8. Photography: setup and processing.
a) Photography setup: wings, scale, label, colour checker, side label (“D”, dorsal); b) cropped wings (.JPEG format); c) .PNG images used as input in *recolorize*.

3. Image Processing

Individual wings were selected through a batch process in Adobe Ps used to crop and export in JPEG format (.JPEG) (Fig. 8b). From each individual, only one hindwing (*HW from now on*) and one forewing (*hereafter referred as of FW*) were acquired, based on integrity; left wings were transformed via horizontal flip in Photoshop to get same orientation as right ones for homologous landmarking (required for the alignment).

Green background was automatically removed from single images with "magical eraser" (threshold = 100) in Adobe Photoshop (Adobe Photoshop CC 2019), after that it was possible to save them in PNG format with transparency, without any coloured pixel outside the wing area (Fig. 8c). All the process was batched to save time (Chained functions: "magic eraser" and "rapid export as PNG").

Some wings required further processing: ruined areas where scales came off were recoloured (stamp clone function in Adobe Ps) only where it was possible to assess the contour of the pre-existing colour. Comparison with the other wing of the same individual was also employed to avoid errors.

4. Image Analysis in R

The pattern analysis was carried out in R (Rstudio), combining the functions of two recently developed packages for animal colour pattern analysis: *Patternize* (Belleghem et al., 2019) and *Recolorize* (Weller et al., 2022). Starting from two workflows already written by the authors, I combined Patternize and Recolorize tools in a hybrid workflow (in Appendix) to produce a PCA quantifying colour pattern variation, and accurate measures of wing melanization (proportion of black on total area). By analysing the pattern variation in a quantitative framework, it was possible to objectively capture subtle pattern changes across the entire wing surface, considering multiple axes of trait variation at once, in a multivariate trait analysis, rather than simple discrete trait changes (Bainbridge et al., 2020).

I decided to utilize the package Patternize that gave as result an intuitive principal component analysis of pattern shapes variability, where pattern was treated as a multivariate trait, processing different types of shape variation at once. At the same time, I found Recolorize more intuitive and efficient in handling colour maps generation for the study species, under sub-optimal conditions, where sampled individuals can often present imperfections due to abrasion and the structure analysed is prone to shape distortion during conservation (e.g., antero-posterior stretch or compression). Specifically, I used Recolorize to generate reliable colour maps, exploiting the package built-in functions to optimize them doublechecking clustering results, refining pattern extraction, and performing minor one-by-one image manual edit.

4.1 Pattern extraction – Patternize&Recolorize workflow

The first phase of the pattern extraction required landmark positioning, that was carried out in ImageJ. Scale setting was not required for the pattern analysis, as subsequent alignment in R was done as Procrustes fit, consequently melanization was assessed as a proportion.

For each wing homologous landmarks were manually set at wing veins intersections, nine on FW and ten on HW (Fig. 10). The landmarks map was designed by me, without precedent example found in literature for this genus, after resulting adequate in the trials. All the landmarks were set on veins intersections, as these are shared and invariable structural elements of the wing morphology. Moreover venous junction points on the wing can provide positional information, anchoring the primary characters to one region of the wing (Gawne & Nijhout, 2020). No landmark position was assessed based on presumably conserved shape of colour pattern (i.e., center of the central white spot in FW), because that would have not been independent from the variable I wanted to measure, the pattern. Both external landmarks (vein ends on the perimeter) and internal landmarks (internal vein crosses) were used. For each wing type (FW and HW) a reference outline was drawn, to define the region of interest, on the perimeter of the reference image to which all the others were then aligned and stretched. Landmarks were saved as XY coordinates in text files, with the same

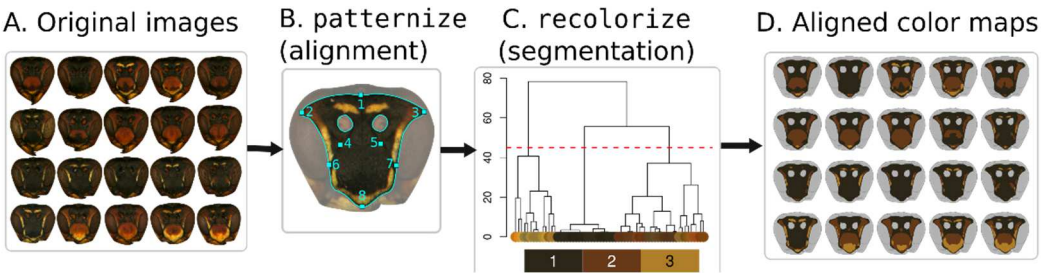

Figure 9. **Image Alignment and Colour segmentation.**
First half of the image analysis workflow: A) The input is a group of original images without background (.PNG); B) Alignment step with a function from Patternize; C) Pixel binning by colour and clusterization with a function from Recolorize; D) Output: aligned images recoloured with a limited number of shades.

Figure 10. **Homologous Landmarks.** Forewing and Hindwing (right, left).

exact name of the images they refer to (i.e., FI21.2-35.4_dfwR.txt are the coordinates of the image FI21.2-35.4_dfwR.PNG); the two outlines were also saved in text files.

The method followed the workflow in Fig. 9, adapted from the one reported in Example D of Weller et al., 2022, working with both Patternize and Recolorize.
The function *alignLan()* of the Patternize package performs the automatic alignment on the reference (target) image and the background cropping following the outline polygon. This step is analogue to the Procrustes fit of geometric morphometrics; hence it removed the variability in dimension, orientation, and shape of the wings, homogenizing the base. On top of that, function *alignLan()* does not generate aligned images based on original aspect ratio (Width x Height), but use a default square shape, so I needed to define the expected aspect ratio of the resulting aligned image (field: res=c(W,H)). Measured aspect ratio (W/H) was used to set output dimensions: 1.6 for FW reference and 1.1 for the HW. I used PNG images with transparency, to avoid sampling background pixels when the wing frame is smaller than the outline, that would bias the pattern area values.

The second step is the image segmentation by colours, using Recolorize functions*: blurImage(), recolorize2(), thresholdRecolor(), recoloredImage(), absorbLayer()*.
Function *blurImage()* was used to attenuate interference of light reflexes in the continuity of colour patches (see Weller et al., 2022). Given a group of aligned images, the function *recolorize2()*, firstly bins all the pixels in a defined number of colour clusters, then proceed merging clusters by similarity down to a number of hues defined by the user. In this case the wings were segmented in two colours (black and yellow or white). *thresholdRecolor()* served as necessary refinement step for colour sampling.
Through the function *recoloredImage()* bicolour images were obtained, with pixels coloured in accordance with the two-colour palette generated, based on assigned cluster. I used aligned *plotImageArray()* function to visualize (plot) colour maps, to proceed with evaluation of the colour segmentation accuracy by eyes, with the original images as comparison. This step was fundamental to spot errors in the alignment and incongruency in the colour picking. Where single images resulted visibly different from the original due to wrong assignation of colour, possible in ruined areas, *ad hoc* pixel re-clustering was performed, customizing the settings until colour segmentation was acceptable. *absorbLayer()* function was used as last resort on single recoloured images to remove mis-attributed areas of a set maximum size "x", because when run on the whole sample repeatedly caused "*Aborted session*" issue in R.
After evaluation, recoloured aligned images were exported as JPG (customized function *expRC_JPG()*, see Appendix).

4.2 Analysis of melanization pattern variation

After delimitation of the pattern patches, recoloured images were used as input in the proper pattern variation analysis using Patternize workflow (Fig. 11).
The first step consists in the alignment of images as a stack of raster layers through *patLanRGB()* function: the function performs both the alignment and the pattern extraction at the same time. Although all the images were already aligned at that point, since the function necessarily requires a set of landmarks, new landmarks and outlines were set for recoloured images. I set four landmarks to define the boundaries of the region of interest and these coordinates were the same for each image, since they were already aligned. To shorten this redundant landmarking process I created the function *RC_lm_listing()* (in section Appendix): for each wing type a .txt file with four landmarks was saved; the function would generate an "*x*" number of copies (equal to images number) of the first .txt file, each renamed after a different image ID.

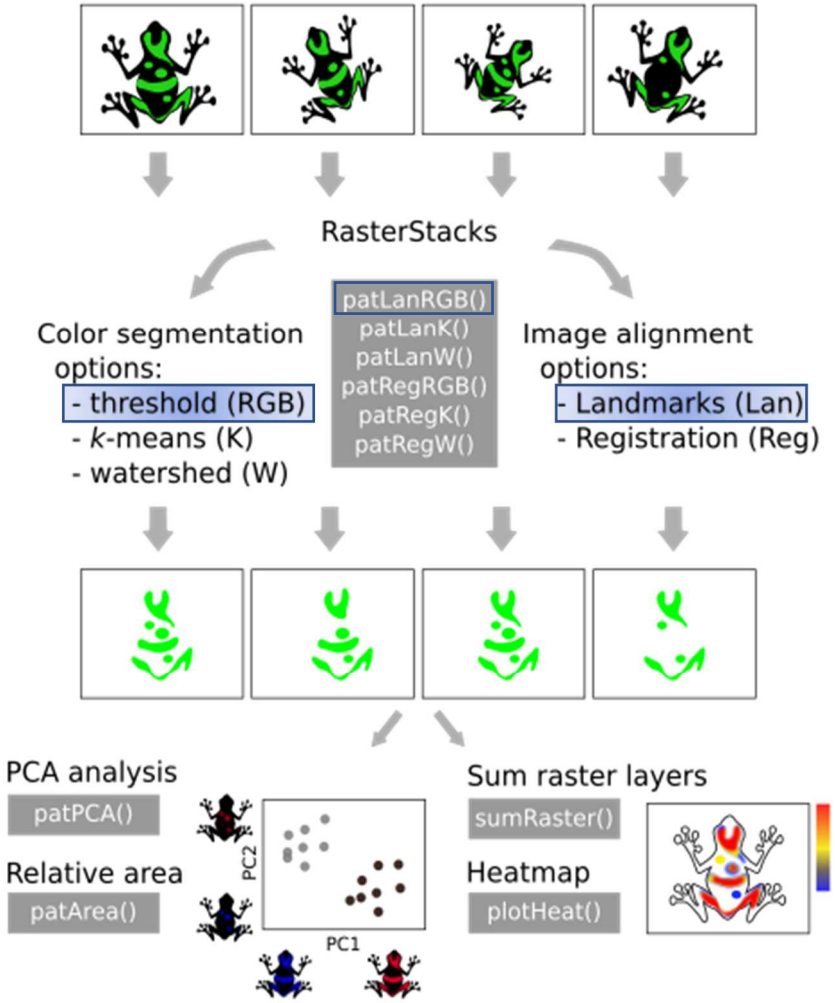

Figure 11. Patternize workflow for pattern analysis (Belleghem et al., 2019).
Second part of the image analysis: pattern extraction and data analysis. Images are aligned using landmarks and segmented by colour with RGB threshold (*patLanRGB()*), to generate a raster stack. Pattern variation can be visualized through an heatmap (*plotHeat()*); PCA analysis is performed automatically on shape variation (*patPCA()*) and pattern area can be extracted (*patArea()*).

Colour-based segmentation in *patLanRGB()*, to extract the black pattern, required a threshold of RGB values (Red, Blue, and Green) for the targeted pattern colour. RGB values were sampled with Patternize function *sampleRGB()* from an image of the pool (Belleghem et al., 2019). These were 68, 67, and 62 for FW and 88, 82, 70 for HW. "colOffset" was adjusted to 0.05, as confidence interval for the RGB threshold, to account for the variation in melanic black hues. "adjustCoords" field was set as "FALSE", to save time, as there is no actual need for alignment of recoloured images (landmarks used only to define boundaries). Patternize use these values to extract the presence and distribution of melanin across the wing: wing images were reduced to matrices of pixels with binary values, "1" corresponding to pattern colour and "0" to the background colour.
Afterwards, an heatmap was generated, with the function *plotHeat()*, to get a map of variability of the region of interest, in which each pixel of is assigned a value (translated to a chromatic scale) equal to the proportion of wings in which that pixel is marked as "1", presenting the pattern.

Lastly, the PCA on melanization pattern was performed through the function *patPCA()*; the variation extracted is plotted, allowing me to examine the patterns of variation and covariation among the black pattern elements. While storing the PC in a variable, the function *patPCA()* automatically plot PC2 on PC1, with respective proportion of variance explained. In addition to that, on the axis' sides are shown the areas of the wing that varies along the component, represented in two wing outlines by highlighting regions that varies between the two extremes phenotypes of that PC axis (Fig. 11). This smart representation allows to directly assess the area that is considered by each PC, in order to better define the nature of the overall pattern variation present.
In addition to shape analysis, relative pattern coverage was quantified with the function *patArea()*, that would give the relative area of the melanic pattern.

4.3 Parental wings analysis

Parental wings were analysed only afterwards, separately, to avoid influencing the principal components analysis with their variability. For hindwings only paternal wings were used; the main reason is that female melanization is very different from male one, so we did not have options of direct comparison. Furthermore, female's hindwings in the sample were in worse conditions, rarely usable, due to folding. For forewings a father-offspring regression was performed to produce an output comparable to the hindwing regression.
After pre-processing of the pictures and landmarking, the pictures were processed in R along with the same reference image from the offspring samples, to grant the same alignment and cropping without spending time in re-aligning the same offspring wings. Pattern coverage was obtained through *patArea()* (Patternize).

5. Statistical Analysis

All statistical analyses were carried out with the software R v. 4.1.1 using the RStudio v. 1.2.1335 interface. The level of significance in all analyses was set at $p < 0.05$.

First, basic descriptors of distribution of melanin coverage (min, max, mean, sd, range) were extracted with *summary()* function (base R) for each group of the following hierarchical partitions: Phenotype (two levels), Genotype (three levels), Family (12 Levels). Each partition was then tested for difference in melanization means, to look for group-specific values of pattern coverage, through the base R statistic tools *wilcox.test()* (on Phenotypes) and ANOVA – *oneway.test()*, not assuming equal variances – for multiple means (Genotype and Family). Families' distributions were used to acquire more detailed information about the melanization variability within colour genotypes: since variation in offspring melanization within and between families of the same colour genotype would derive from genetic variability uncorrelated to colour locus. Second, the analysis of pattern shape variation and its correlation to hindwing colour phenotype and colour locus genotype was performed exclusively with the tools provided within the Patternize R package.

In addition to that, I performed a sire-offspring regression on wing pattern coverage (for both wing types) to estimate the broad-sense heritability of the trait, proportional to the genetic component of its variance. Midparent-offspring regression was not possible on HWs because female HWs were in bad condition and FW sire-offspring regression was better comparable to HW estimation. First, the average pattern expression of a family (proportion of black coverage) from known sire was calculated (Nokelainen et al., 2013). Then, the melanization (quantitative) of progeny was regressed against the coverage of the sire pattern in linear regression. The obtained heritability estimates then equal twice the slope of the single-parent mid-offspring regression line (Lynch & Walsh, 1998). Lastly, the reaction norm was obtained with the function *stat_poly_eq()* of the package "*ggpmisc"*, an extension of *ggplot2* package.

Phenotypic frequencies of the pedigree were extracted directly from to the 24-generation pedigree of stock population reared across 9 years at Jyväskylä University facilities.

RESULTS

1. Wing Pattern Coverage – Wing Melanization

Wing pattern coverage values, hereafter referred as “wing melanization” or “melanization” obtained as proportion of the wing frame covered by the black pattern are collected in Tab. 2 and plotted in Fig. 12.

Hindwing in the sample analysed showed a range of melanization from 21 to 70 per cent with a mean of 50% of black coverage (Fig. 12, Tab. 2a), exactly matching what previously reported for European male populations (Hegna et al., 2013).
As we analyse hindwing melanization (pattern coverage), we can clearly see some kind of bimodal distribution of the specimens, that reflect the two currently adopted categorization for the phenotype, *plus* and *minus*, here with a threshold set at 35% melanization (Fig. 12. See also distribution based on pattern shape in Fig. 19). It seems that even in families showing both types of offspring, like family n.42 and n.35, the threshold area is avoided, forming a discontinuity. These heterogeneous families are expected to hold enough variation in their genome and/or plastic response to express these values, yet in the interval between 30 and 40 per cent melanization fell only four individuals out of 120 (Fig. 12), whereas in any other 10% increment sector there are at least 18 individuals (sector 20 to 30%).
Forewing showed a narrower range of variation, from 60 to 83 per cent, with an average melanization of 73% and a continuous variation (Table 2). The overall correlation between forewing and hindwing degree of melanization was tested high and positive at 0,82 ($p<0,001$). When analysed by partitions, the group of *minus* melanin phenotypes was the only one showing no correlation between FW and HW melanization. Although *minus* tested were only yellows, colour was not the discriminant as the *plus* yellows shown the highest correlation (0,89; $p<0,001$).

Contemplating a third melanization class makes sense in light of the measured range of HW and overall pattern coverage variation attributed to the two categories, in which the “minus phenotype” describes a range of 15% pattern area proportion (roughly from 20% to 35%), while “plus phenotype” entails a 30% range of variation (from 40% to over 70%). This spread can also be seen in the approximate measure of overall melanization, calculated as mean proportion between the two wing types, where phenotype held twice the variability showed by *minus* group. Nevertheless, in first place the variation observed in overall coverage did not present any significant bumps; secondly, there were some cases in which HW melanization did not correlate to FW’s, hence it did not reflect overall coverage.

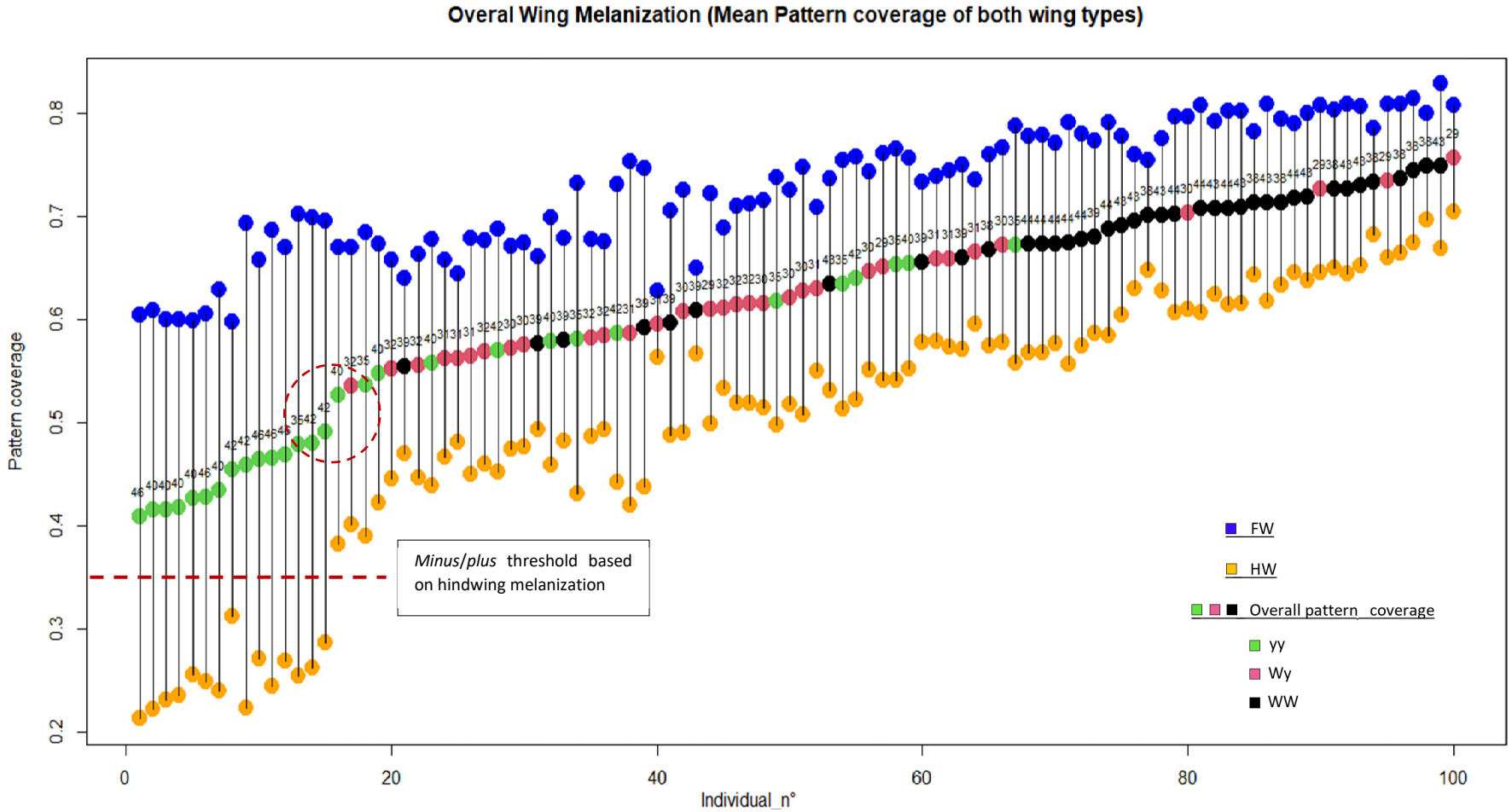

Figure 12. Melanization as proportion of wing frame covered by pattern. Individuals (x-axis) are organized in crescent order of "overall melanization" (arithmetic mean of FW and HW), the series of values in the middle, coloured by genotype; family number is shown above each point. Forewing (blue) and Hindwing (orange) melanization values are shown. The red-dashed line allows division of all *minus* from *plus* individuals. The dashed circle shows a discontinuity in overall melanization that perfectly overlap with the "+/-" categorization.

Figure 13 Aligned Recoloured forewings.

Figure 14. Aligned Recoloured Hindwings.

1.1 Phenotypes

Average hindwing melanization level in white individuals was significantly higher than in yellows, respectively 56% and 37%. Phenotypes shown overlapping (Fig. 15a-b), but different distributions for this trait (p<0,001, Tab. 1*a*). An important feature of the sample is that *minus* phenotype was carried mostly by yellow individuals, half of which (19) were "*minus*", whereas just one white *minus* was reported. To mention, the only white minus phenotype was not an aberration, since another similar specimen was found in the sample but not utilized because of bad conservation state.

Forewing showed a similar trend, with higher melanization in whites (75%), than in yellows, 68%. The difference is statistically significant (p<0,001, Table 1b), but the distributions overlap even more than for hindwings (Fig. 15c).

Overall, no melanization feature was found, neither in HW nor in FW, to be exclusive of a phenotype, although *minus* HW phenotype in this sample was shown mostly by yellows.

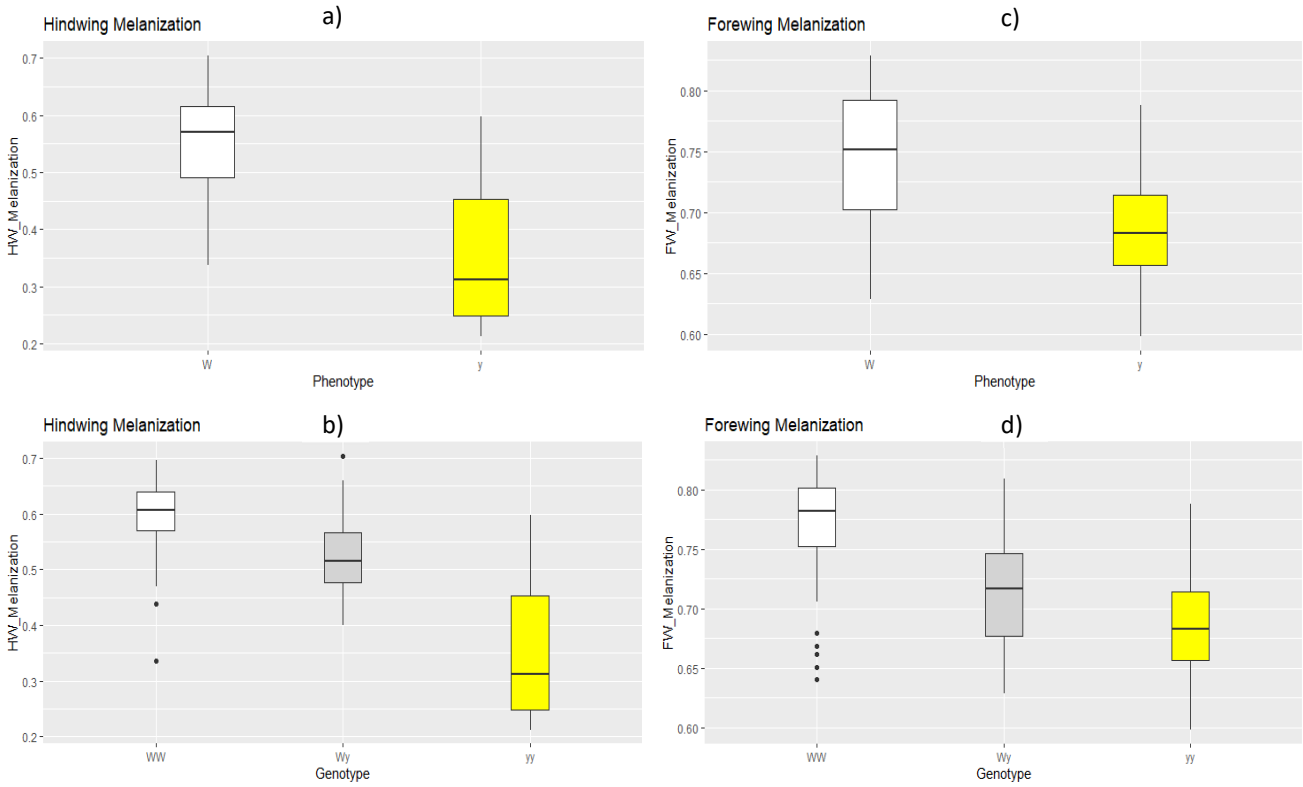

Figure 15. Melanization trait distributions.

Boxplots of Hindwing (a,b) and Forewing (c,d). with phenotypes (a,c) and genotypes (b,d).

1.2 Genotypes

Genotype-wise, among the hindwings, white homozygotes had the highest average pattern coverage of 59%, followed by heterozygotes (52%) and yellows (37%) (Fig. 15b). All means are significantly different from each other ($p<0,001$, Table 2a). Noticeably, within white phenotype the more melanized individual was a heterozygote (Wy), while the lowest melanization was on a homozygote (WW); these values are opposite to what we could expect from observing the average melanization values, by which melanization of WW was higher than Wy.

Forewings showed more extensive overlap in melanic coverage between genotypes than HW, but difference in means still resulted statistically significant by Anova test (Tab. 2b). In the FW plot (Fig. 15d) it can be seen as homozygotes white occupy the more melanized region, the yellows are concentred at lower values and highly variable heterozygotes are in the middle, almost spanning across the whole distribution.

a) Hindwings

Colour	Genotype	Family	mean	max	min	sd	var	range
W 0,559	WW 0,524	**29**	0,582	0,705	0,478	0,078	0,006	0,226
		30	0,512	0,610	0,456	0,050	0,002	0,154
		31	0,523	0,595	0,420	0,062	0,004	0,175
		32	0,479	0,533	0,401	0,041	0,002	0,133
	Wy 0,593	**38**	0,649	0,697	0,575	0,034	0,001	0,122
		39	0,508	0,587	0,337	0,078	0,006	0,250
		43	0,623	0,669	0,531	0,035	0,001	0,137
		44	0,592	0,646	0,557	0,027	0,001	0,089
Y	yy 0,354	**35**	0,442	0,558	0,254	0,111	0,012	0,303
		40	0,350	0,552	0,222	0,117	0,014	0,331
		42	0,379	0,597	0,223	0,128	0,016	0,375
		46	0,244	0,271	0,212	0,021	0,000	0,059

b) Forewings

Colour	Genotype	Family	mean	max	min	sd	var	range
W 0,744	WW 0,721	**29**	0,582	0,705	0,478	0,078	0,006	0,226
		30	0,512	0,610	0,456	0,050	0,002	0,154
		31	0,523	0,595	0,420	0,062	0,004	0,175
		32	0,479	0,533	0,401	0,041	0,002	0,133
	Wy 0,767	**38**	0,649	0,697	0,575	0,034	0,001	0,122
		39	0,508	0,587	0,337	0,078	0,006	0,250
		43	0,623	0,669	0,531	0,035	0,001	0,137
		44	0,592	0,646	0,557	0,027	0,001	0,089
Y	yy 0,684	**35**	0,442	0,558	0,254	0,111	0,012	0,303
		40	0,350	0,552	0,222	0,117	0,014	0,331
		42	0,379	0,597	0,223	0,128	0,016	0,375
		46	0,244	0,271	0,212	0,021	0,000	0,059

Table 1. Melanization values (proportion of wing covered in black). a) Hindwing values of average coverage within families; b) Forewing values of average coverage within families.

a) Hindwings

Wilcox.test	W	p
Phenotypes	2774	2,00E-12

b) Forewings

Wilcox.test	W	p
Phenotypes	2447	5,20E-07

Hindwings ANOVA Table

Partitions	df	F	p
Genotypes	2	51,4	1,30E-14
Families	11	118	8,70E-28
W_Fam	7	20,1	5,90E-10
WW_Fam	3	12,1	8,40E-05
Wy_Fam	3	4,3	1,70E-02
yy_fam	3	13,3	1,30E-04

Forewings ANOVA Table

Partitions	df	F	p
Genotypes	2	31,5	1,00E-10
Families	11	38,4	4,80E-18
W_Fam	7	38,8	1,90E-13
WW_Fam	3	10,5	2,30E-04
Wy_Fam	3	16,1	2,70E-05
yy_fam	3	10,7	2,80E-04

Table 2. Statistical tests' results. Results of Wilcoxon and Anova tests between different partitions of HW (a) and FW (b). All values are significant.

Correlation tests between FW and HW melanization were carried out for each genotype, white homozygotes (0,75; p<0,001), heterozygotes (0,74; p<0,001), yellows (0,81; p<0,001).

1.3 Families

The sample showed ample variability in the trait values distribution among and within colour families (Fig. 16). Families of the same colour genotypes can greatly differ in melanization, in both their mean and their variance, moreover, families from different genotypes can be more similar between each other than with families of same genotype.

ANOVA (*oneway.test()*) on overall difference in family means revealed significant differences in average melanization value between families. What's more, within the same genotypic class, families were found to significantly differ in melanization means and range of variation. For example, if we compare 2 yellow families (yy), family n. 46 had an average hindwing melanization of 24% and range of melanization of approximately 6%, while family n.42 shown a mean of 38% with a range of variability of 38%, from 22 to 60 per cent coverage (Tab. 1a; Fig. 16a). Forewing variance was smaller, still in WW genotype family n.44 has mean 79% and range of 4 percent point, while family n.39 has mean 70% with a 13 % range (Tab. 1b; Fig. 16b).

There are some salient information about intra-family variance that can be extrapolated from the two plots: 1) Both wings can be consistently different in average melanization also between families of the same genotype; 2) For both wing types there was a huge variability in intra-family variance, with some extremely homogeneous families, and others more spread on the melanization scale; 3) The entity of this variance did not depend on colour genotype since each of them shown both very homogeneous families and very heterogeneous ones.

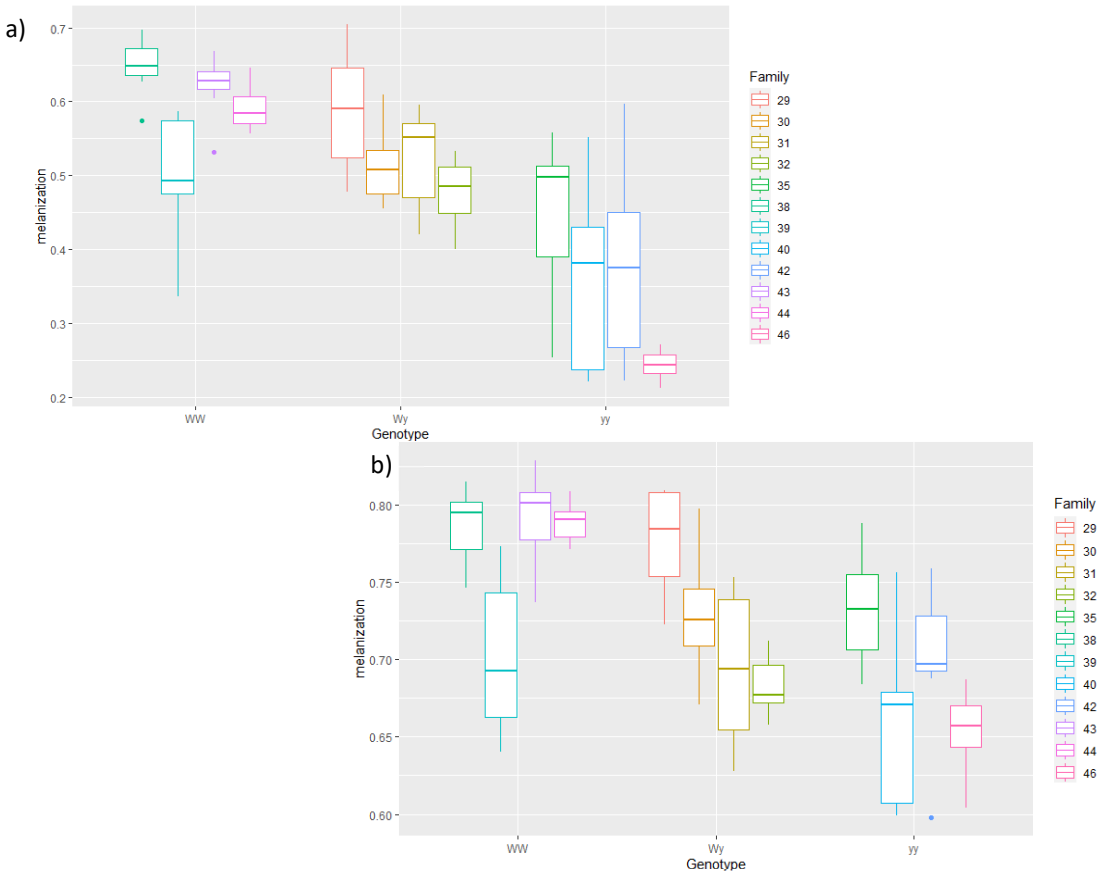

Figure 16. **Family distributions for the trait melanization**.
Boxplots with Hindwing (a) and Forewing (b). Families are grouped by genotype (on x-axis)

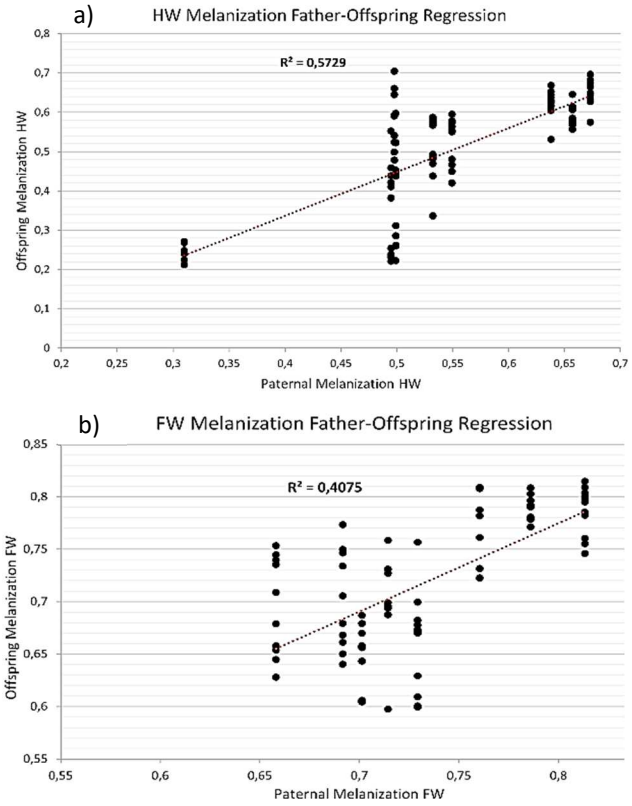

Figure 17. **Father-offspring regressions**. a) Hindwings and b) Forewings.

1.4 Sire-offspring regression

Overall, less melanized sires gave birth to less melanized sons and from more melanized fathers originated more melanized sons, for both wing types. HW melanization appeared more heritable, while FW offspring values are less clustered, especially at lower values.

The father-offspring regression of hindwings gave an R^2 equal to 0,57 (F = 118, df = 88, p-value < 2.2e-16); doubling that value, I obtained a heritability estimate of h^2 = 1,14. The fact that estimated h^2 for HW melanization exceeds "1" is a problem, since 1 is the maximum meaningful value of h^2, that poses a limit on the conclusions we can draw. Forewing's father-offspring distribution is also that the trait is heritable to certain extent in father's lineage, with R^2 = 0,41 (F = 52.28, df=76, p-value = 3.225e-10) and an estimated heritability of h^2 = 0,82. Although the trait ("melanization" as pattern area) seems to be heritable for both HW and FW, no strong statement should be done since come values are off scale.

1.5 Pedigree analysis

Partition	**Phenotypes**		**Genotypes**			**Number of *minus* individuals**
	W	**Y**	**WW**	**Wy**	**yy**	
% *Minus* 2013-2021	26%	62%	2,9%	30%	62%	W_=3251* yy=5659 WW=59 Wy=1621
% *Minus* 2013-2014	37%	60%	*NA (*)*	40%	62%	W_= 589* yy=763 WW=2 Wy=289
% *Minus* 2019-2020	8,0%	54%	2,5%	10%	54%	W_=281* yy=770 WW=32 Wy=115
% *Minus* in generation 21.1	1,1%	49%	1,5%	1,4%	49%	W_=12 yy=277 WW=6 Wy=6
% *Minus* in this study (21.2)	1,2%	51%	2,3%	0%	51%	W_=1 yy=19 WW=1 Wy=0

Table 3. ***Minus*** **individuals by sub-samples of the pedigree.**
Number and proportions of minus individuals across years. Sum of WW and Wy does not represent the total number of W_ (white individuals) in presence of ungenotyped individuals. WW proportion for years 2013-2014 (*) was not calculated because of too scarce number of WW with respect to ungenotyped ones.

Pedigree analysis based on the two categories of hindwing melanization revealed that *minus* phenotype expression greatly differs between colour morphs: yellow males carried the least melanized phenotype in more than 60% of the cases, whereas whites had a frequency of 26% over the entire time-period. Difference in proportion of minus was evidenced also between the two white genotypes, with 30% of *minus* Wy males against 3% of *minus* WW individuals (Tab. 3).

Since phenotypic frequency did not match the ones in the sample in this study, macroscopic phenotypic oscillations were checked by comparing minus phenotype's frequency in the first two years of rearing (five generations across 2013 and 2014), with the generations of the last two years (six generations across 2019 and 2020). In the first 5 generations, across years 2013 and 2014, there were 588 white minus over 1621 white males (37%), whereas in the 6 more recent generations (years 2019 and 2020) the number drastically decreased to 282 over 3442 (8%). Yellows showed very limited variation between the extremes, going from 60% to 54% in the same aforementioned generations. One key aspect to consider is that discrimination between WW and Wy was not fully in use for many years: until 2019 there are almost no traces of WW genotype, with only 56 individuals marked as "WW" and the rest was marked as "W_" or "Wy". For that reason, WW genotype values before 2019 cannot be considered.
Lastly, the first generation of year 2021 presented a white minus frequency of 1,1% (with over 1000 white males) and a yellow minus frequency of 49,3%, closely resembling frequencies shown by the sample used in this study (W, 1.2% minus; Y, 51% minus). Key aspect in considering the sample is the non-random method of sampling, in which priority was given to sampling the whole phenotypic distribution, with less focus on preserving phenotypic frequencies of the families. Regarding that, only one more white minus was spotted in the entire sample, but in bad conditions, hence left out.

2. Pattern Analysis – Patternize PCA

The PCA outcomes from the pattern analysis are represented in Fig. 19 and 21 for hindwings, and Fig. 23 for forewings, as output of *patPCA()* function of Patternize.

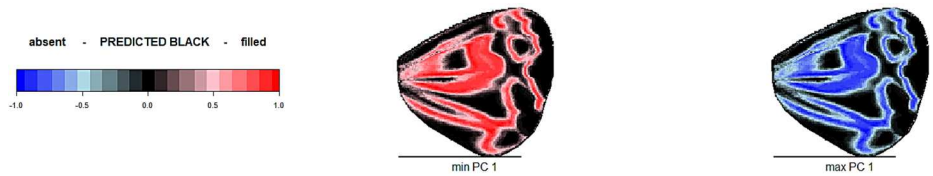

Figure 18. Explanatory figures from *patPCA()* output. From left: Legend; PCx min value; PCx max value.

The explanatory figures on the side of the axis represent the area that changes its black coverage along the that specific PC (see reference example in Fig. 18). The extremes of the PC distribution are plotted with the colour markings referring to prediction on pattern presence. Following the legend in Fig. 18, black stands for regions that are not changing their colour across the sample, being either melanic or background. Red represents a positive increment in black coverage, so that the wings on that edge of distribution would present all the area melanized. On contrary, blue stands for a depletion of black pigment, so that the wings in that area show the only background colour (white or yellow) in that area. Intensity of the colour is the "predictive power" on the particular change in melanization, so the correlation between PC value and the marked change across the sample; it

depends on the proportion of wings at the same PC value that present the same phenotype.

2.1 Hindwing

In the hindwing the first two PC explain 36,6% of the total variance, respectively 29,2 and 7,4 per cent each. PC1 divide the group visibly in two clusters, with an empty sector at 20<PC1<30, whereas no evident points disjunction is present along the PC2 axis.

The PC1 catches the variation in overall hindwing melanic coverage, the correlation between these two resulted extremely significant and high (-0.995).
In all the variable area, the changes in black pattern elements are coherent with increment and decrement in width of the stripes and dots, inversely proportional to the PC1 value. There is a reduction in melanization across the whole variable area from highly-melanized low PC1 values to less melanized high PC1 values. The PC efficiently distinguish the samples according to the categories "plus" (low PC1 values) and "minus" (high PC1 values) used in laboratory to describe the phenotype, showing a bimodal distribution of the points (Fig. 19). In proximity of the threshold, intermediate PC1 values are under-represented in the sample.
Disproportional coverage of specific areas, at cost of contraction elsewhere, was not registered by this PC, therefore PC1 could be considered a good proxy of melanization phenotype, without any additive information on pattern properties.

The second principal component (PC2) axis highlights more complex shape differences in the hindwing bands among the samples. Noticeably at genotypic level we can observe a partial clusterization of WW (in black) at lower PC2 values

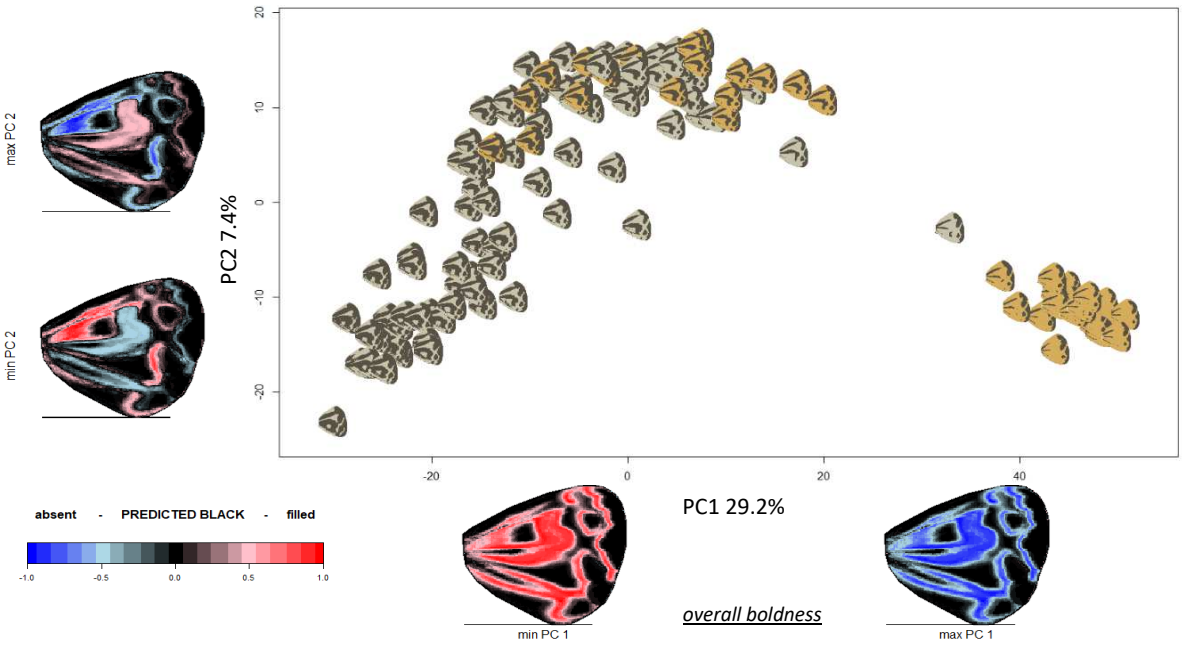

Figure 19. *patPCA()* output of hindwings.
PC2 plotted over PC1**.** Recoloured wing pictures are plotted one the respective PCA coordinates.

than heterozygotes, Wy. This PC represents a contrast, a disproportional deposition of pigment in some areas and not in others, or even a reduction of some pattern elements at the enlargement of others. PC2 values appear proportional to the ratio of coverage in area "2" (hereafter, "above-hook melanization", or "AHM") over the melanization in area "1" (Fig. 20).

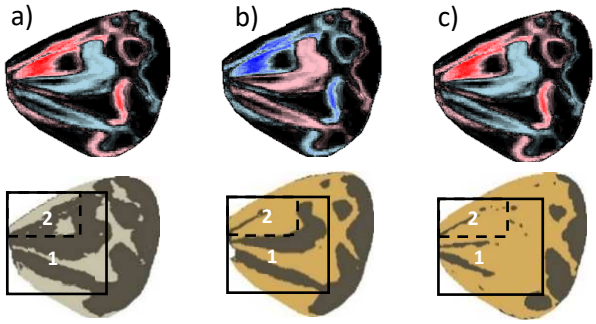

Figure 20. **Variance in Pattern shapes along PC2 axis** (in Fig. 19).
First row: images generated by PCA. Second row: recoloured images that show the corresponding PC2 values: a) *plus*, b) *plus*, c) *minus*.
The square entails most of the variable area on which PCA is based. The small rectangle - "Sector2" - highlights a region of interest, the area above the hook.

Minus individuals show the same amount black colour in the top left corner as some *plus* phenotypes, but thinner central wing stripes, that can heighten the aforementioned ratio. That is the reason why as we plot the proportion of black in the two sections (PC2), *minus* phenotypes (first from the right) fall around the same PC2 values as heavily melanized *plus* wings (first from the left). The key point here is that the first black stripe in the *minus*, as in middle *plus* phenotypes, can be generated by the structural colour of the vein, irrespectively of the number of black scales and it is uncorrelated to it.
Given the radical variation in pattern shapes, the presence of *minus* in the stack made the PC2 controverse and too general in some area: 1) highly melanized *plus* phenotype has low PC2 values that corresponds to the increased coverage of above hook area (Fig. 20 a, in red), but do not show the depletion of pigment from the hook area that is represented in the figure (Fig. 20a, in azure); 2) *minus* phenotype show the same low PC2 values and by consequence the same variation indicator, where hook reduction (Fig. 20 c, in light blue) is truly present, but AHM expansion (Fig. 20c, in red) does not actually take place; 3) medium melanized individuals (Fig. 20b; medium PC1 values in Fig. 19) have high PC2 values and colours representing variation from the individuals at low PC2 are true or false, depending on which group of low-PC2 individuals we are comparing (Fig. 20).

The confounding effects showed in the coloured figures hindered the possibility to rigorously assess the presence of differences within the *plus* group, that is group of interest as we try to uncover discriminant elements between white genotypes (almost exclusively with *plus* phenotype). In the attempt of uncovering differences between WW and Wy, another PCA was run on the sole *plus* phenotypes, to investigate with more precision and sensibility the distribution of the two white genotypes.

In the PCA on the sole *plus* (Fig. 21), it is visible as PC1 in this subgroup is still strictly correlated to overall HW melanization level; the correlation between PC1 and melanization in *plus* phenotype is indeed very high, equal to (-) 0.97. Regarding that, from comparisons with melanization values, it has been observed that PC1 spread the points more than pattern coverage does, exploiting some shape information. The spreading seems linked to proportion of AHM on the total coverage and interestingly it generates more space between WW (black) and Wy (red) individuals along the X-axis, shifting WW on the left and Wy on the right: at comparable black coverage WW are mostly assigned lower PC1 values (left-shift) than Wy (horizontal-shift). This means that in many cases the AHM is relatively higher in WW than in Wy for equal melanization levels (Fig. 21). There are no case in which a WW that has higher melanization than a certain Wy, is assigned a higher PC1 than that Wy individual.

The actual difference from the previous PCA plot is that PC2 is now based on a small and specific area that seems to be conserved for a given PC2 value (high predictive value means homogeneity of the shape at same PC value). When we look at low PC1 values (PC1< -10), for equal values of PC1 between WW and Wy, the first group always present higher PC2 values than the latter. At low PC1 values there is an almost linear relationship between PC1 and PC2 for the majority of WW individuals, such as at low PC1 (high AHM coverage) corresponds low PC2 (high hook boldness)**.** From the combination of PC1 and PC2 it can be demonstrated that WW individuals are reaching higher AHM at lower melanization values, covering the above-hook region (Fig. 20, sector 1) at expense of the hook boldness (Fig 20,

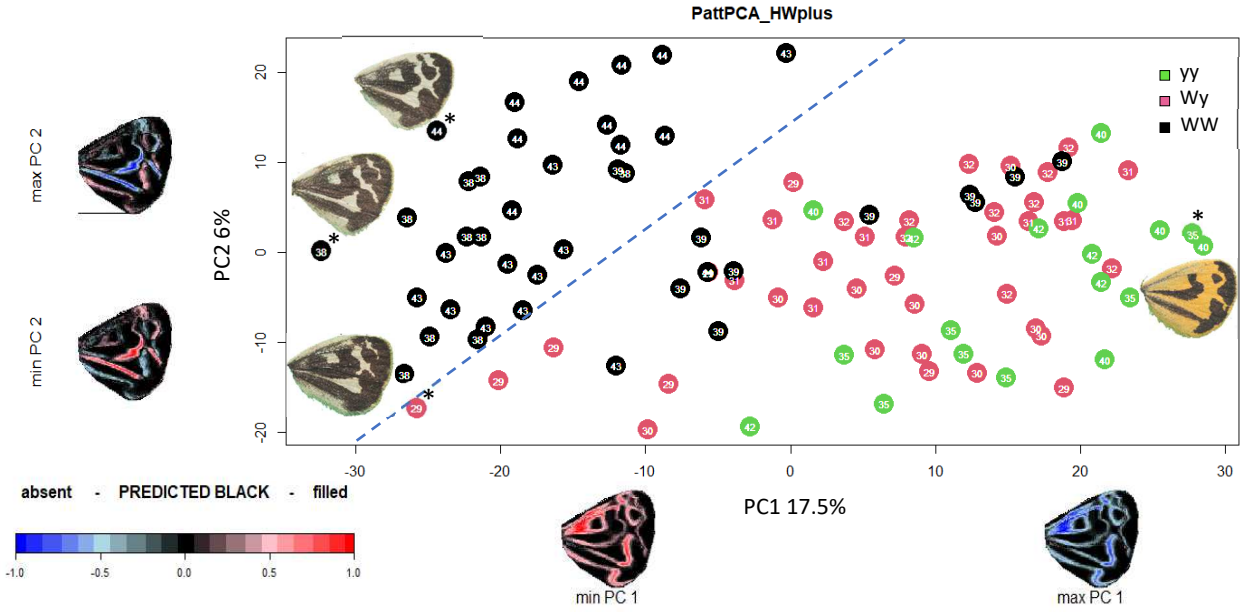

Figure 21. Hindwing PCA of plus individuals.
PC2 plotted over PC1, with family numbers and points coloured by genotype. The dashed line is a possible threshold WW/Wy based on pattern shapes. Asterisks mark individuals whose pictures are shown nearby.

sector 2), whereas Wy showed to further increase the hook boldness with the increase of overall coverage even at PC1<0, delaying AHM coverage.
At high pattern coverage, approximately with melanization above 0,5, the two genotypes in the sample follow two slightly different patterning models, each prioritising the coverage of different areas over others when melanin synthesis increase: the ratio of AHM to hook melanization and also the ration of AHM to overall coverage are expected to be higher for WW individuals, with a steeper linear relationship between the different pattern shapes extension.
Further information was available from the family's distribution (Fig. 21): the distribution overlap in the PCA space is mostly due to one single WW family, family n.39, that is also the only WW family to have individuals with positive PC1 values and positive mean PC1. Other WW families (n.43 and n.44) showed individuals below the hypothetical threshold drawn in blue, yet these families present only one individual each in that region, identifying them more as outliers of the family's phenotypic distribution.
Reconnecting to the issue of *plus*/*minus* categorization based on pattern elements like the hook presence, I gained more information on the correlation between pattern shapes and pattern coverage. Although the "hook" shape presence/absence is used as categorical discriminator between *minus* and *plus* male's phenotypes, it only represents individuals with intermediate level of melanization (Fig. 19): in more melanized ones it can further extend in "horseshoe" or "closed-hook" shapes. In fact, in the analysed population two main shape shifts were recognized across the hindwing pattern coverage gradient:
1) From *minus* phenotype to *plus* phenotype: the initial two tiny stripes in the central wing area expand, with the appearance of the hook shape and elongation of the bottom band, now in continuity with the distal pattern area.
2) From the hook shape to an "expanded hook": melanized scales appears in the area above the hook, the aforementioned "above-hook melanization" or "AHM", generating either a "horseshoe" black shape or, at its extreme, a fully closed black hook with an island of background colour. Unfortunately, the second pattern shift present transitional zone, with the presence of intermediate forms that can cause problems in defining the exact boundaries of that categorization.

2.2 Forewing

For the forewings PC1 and PC2 cumulatively explain 23,6% of the variance, respectively 17 and 6,6%; no apparent clusterization is generated by either PC1 or PC2 in the PC landscape.
The second PC was reputed non-significant in explaining other features of the pattern; after doing some ascertainment, appeared that the pattern variation enlightened by PC2 could represent a by-product of landmarking. A linear wing distortion, by stretching along the proximate-distal axis, would cause the same proximate-distal shift in edges perpendicular to the axis, such as right border

would be enlarged, and left border would shrink (see “artifact” circled in dotted red in Fig. 23a). Comparisons between pictures showed that such a shift is present in between some samples but was not regarded as relevant. The difficulty of homologous landmarking was definitely higher in FW because of a thicker layer of scales that made it hard to spot the perfect veins intersections in some cases and that was shown in these results. Therefore, for the sake of the analysis, the plotting of PC3 was also considered, although with extremely low variance explanation (5,1%) (Fig. 23b).

The first principal component in FW catches the variation in pattern coverage as well, yet without any visible clustering; the correlation between PC1 and melanization resulted extremely significant and high (-0.978). PC3 appears to account for variability in some pattern boundaries, most of them showing proximal-distal shifts as for PC2, however, a small feature in the anterior proximal zone could be important in explaining some of the variance. At low melanization (PC1 > 0) size variation of a small background patch circled in red (along PC3), can separate white heterozygotes from homozygotes, so that they do not overlap (threshold at PC3 = +2: dashed blue rectangle in Fig. 22). Homozygotes are at higher values, showing a smaller patch. Adding family numbers to the points (Fig. 22), it stood out as there is only one WW family (family 39) whose individuals shown PC1 > 0; moreover, the PC3 values of that family remain over the distinctive threshold for each individual across a large PC1 range, whereas other homozygotes surpass it at negative PC1 values.

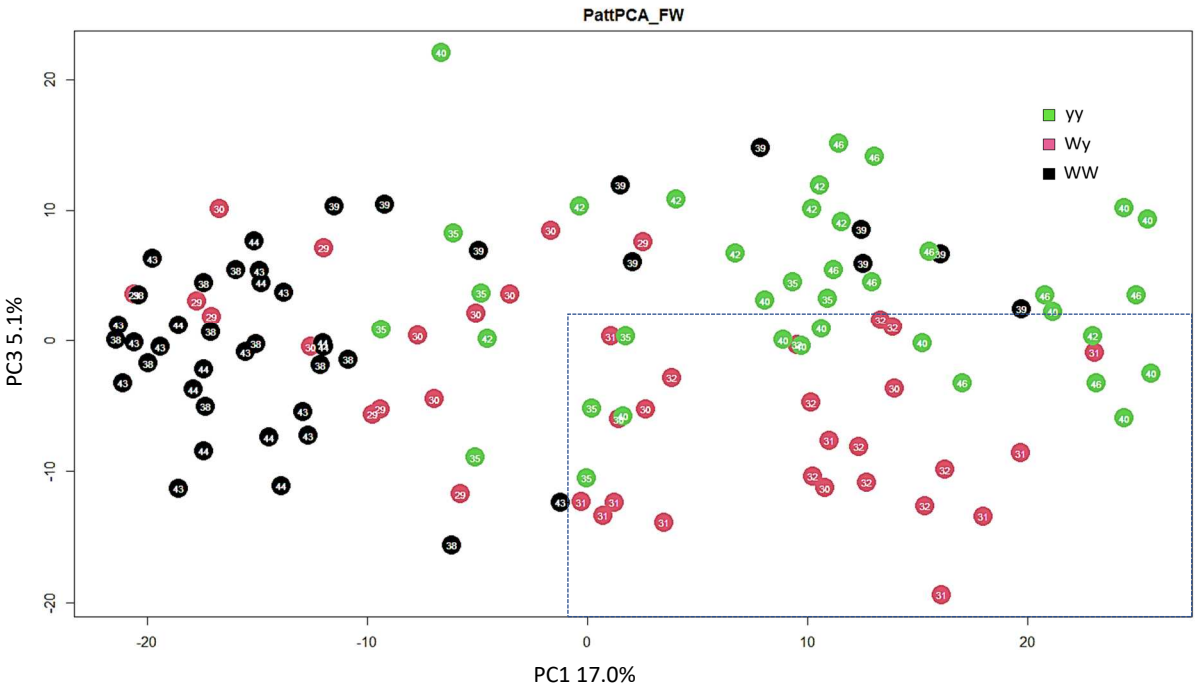

Figure 22. Forewing PCA plot.
PC3 plotted over PC1 with family numbers and points coloured by genotype. Dashed rectangle delimiting an area in which pattern features of the two white genotypes does not overlap.

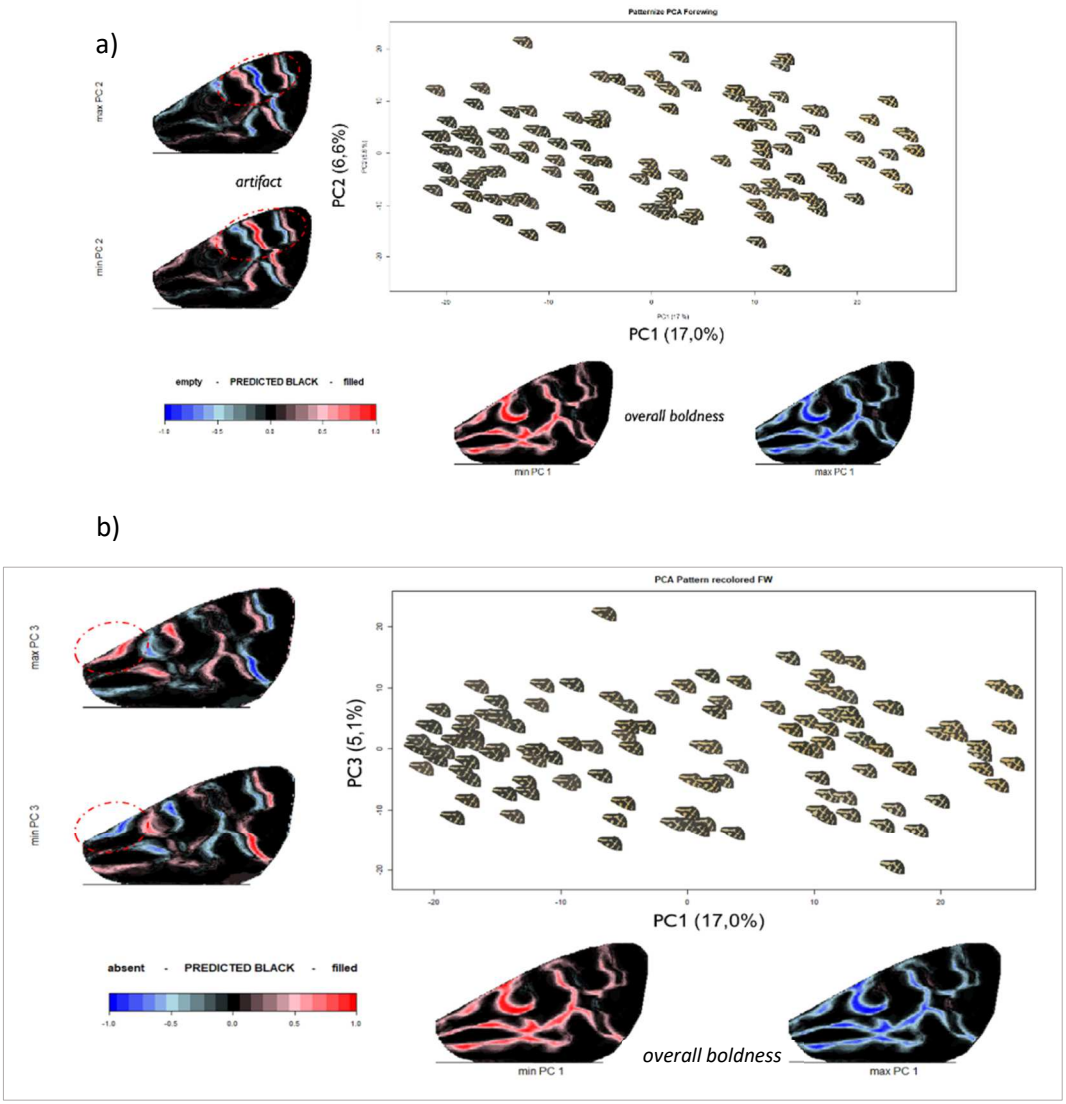

Figure 23. Two forewing *patPCA()* outputs.
a) PCA showing a controversial PC2 (same PC1 on the x-axis), with peculiar variation between extremes, resembling alignment artifact, circled in red. b) PCA plot with PC3 over PC1, an interesting area is circled.

3. Wing Patterning Model

The pattern of forewing in its less melanized form it recalls the "Broken Bands" type defined by Gawne & Nijhout, 2020 (Fig. 24). Considering the shape differences observed by eye, the trend of variation in this stock population of *A. plantaginis* can be described as continuous variation in the banded pattern boldness. The banded pattern becomes less recognizable in the more melanized forms where the expansion of the edges leads to the fusion of the spots as is visible even in other species of the same subfamily (Arctiinae) (Fig. 25). Finally, we do not have strict methods to define the pattern of hindwing since the Arctiid archetype has been defined as a model for forewings. Hindwing pattern variation is continuous and attributable to the expansion of the black patches' boundaries.

Figure 24: Models of banded pattern type. From the left: *Apantesis nevadensis*; *Preparctia romanovi*; *Apantesis tigrina*

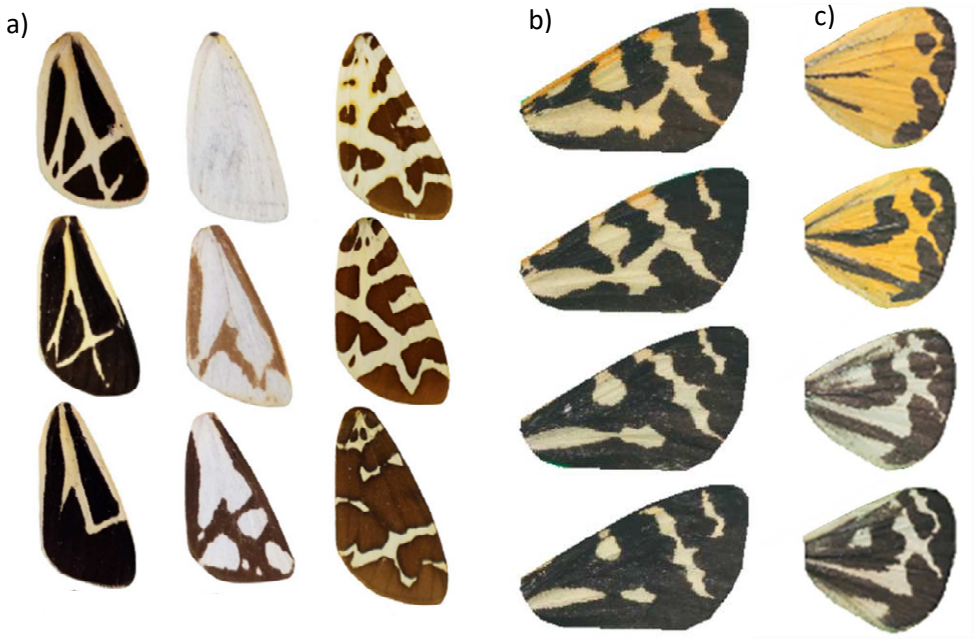

Figure 25. Continuous intraspecific variation in pattern boldness. a) Intraspecific pattern variation of three distinct *Arctinae spp*, from the left: *Apantesis nais*, *Haploa confuse*, *Arctia caja* (Gawne & Nijhout, 2020); b) *A. plantaginis* forewing variability in the sample analysed; c) *A. plantaginis* hindwing variability in the sample analysed.

DISCUSSION

The object of this thesis work was to quantitatively assess the variation in male wing melanization among the Finnish population of the aposematic moth *A. plantaginis* and its potential correlation to the male colour polymorphism.
I found that melanic pattern variation in the sample analysed is mostly due to a sequential enlargement or contraction of the pattern elements boundaries in a continuum, reflecting the overall quantity of melanic pigment synthetised in the wings. Melanization values in the sample and pedigree data revealed a certain degree of covariation between colour locus genotype and wing melanization phenotype (HW and FW). It can be hypothesised that there is an epistatic relationship between the colour locus and the unknown genetic basis of coloration. It was additionally described a putative element for white genotype (WW, Wy) discrimination in HW melanization pattern, although its applicability is to further test.
The binary categorization of overall melanization based on HW was tested efficient and reliable. Although the *plus* phenotype appeared quite variable, finer classification of *plus* individuals based on salient pattern elements appeared not fully reliable at the moment.

1. Black Pattern Shape Variation

From investigation on the different pattern elements, it seems unlikely that intra-populational pattern changes in this species are to be attributed to variation in position of wing pattern primary elements, neither to changes in wing morphology. Conversely, pattern elements appeared “engraved” into the wing plan, anchored to veins paths, varying in their shape boundaries.

If we compare the forewing pattern to the main pattern types found in tiger moths (Arctiinae), what has been observed resemble the characteristics of both *broken bands*, previously described by Gawne and Nijhout, 2020. In our sample, least melanized individuals show a clearer banded pattern type, with interconnected vertical and horizontal stripes of background colour. That was already described in some Alaskan populations as “Cross” phenotype, from the white cross produced in the distal half (Hegna & Mappes, 2014). In more melanized individuals the shapes start to merge, and the original banded pattern is less recognisable, with extinction of some background patches connecting adjacent coloured stripes. The same form, already found in Alaskan populations, was named “Spot Hash” (SH) phenotype (Hegna & Mappes, 2014). *A. plantaginis* showed a trend of continuous variation in pattern “boldness” that finds greater evidence in Alaskan populations of this species, which showed a larger FW melanization range (Hegna & Mappes, 2014). Overall, previous studies on *A. plantaginis* population diversity in alpine and Alaskan regions clearly show the potential further extension of that black pattern

to almost all the forewing area. This generates a quite unrecognisable banded pattern, almost resembling the "bold" type, that is not observed in Central and southern Finland populations (Hegna et al., 2013; Hegna & Mappes, 2014). Given the higher homogeneity of Central and Southern Finnish populations, with respect to Alaskan populations, FW pattern differences in term of disruptiveness within our stock appears shallow, therefore is not expected to produce differences in fitness linked to that defensive strategy. FW pattern variability is even less likely to determine differential fitness benefits between morphs from an evolutionary standpoint. For that reason, an interesting research target for the future can be the expansion of our pattern analysis to Northern Finland populations, to complete the picture of Finnish variability.

At the moment, the Arctiinae archetype and its specific pattern types have been defined only for Arctiinae's forewings, hence, no direct comparisons on pattern types can be done. Although variation in hindwing pattern are extensive, giving the false impression of presence of two distinct patterning developmental schemes, in reality, shapes covaries with the total amount of black pigment deposited, as it has been reported for many tiger moth species (Gawne & Nijhout, 2020). Some areas of the HW pattern are covered in pigment even at low levels of melanization (i.e., distal border). The progressive filling of areas, from the least covered to the most melanized specimens, is consistent with increase in overall coverage and follows shapes that are already "drawn" on the wing, just not coloured at melanization level below a certain threshold. In this species' hindwings the stripes in the central wing area are the most changing pattern elements and they always follow the veins' path. To give an example, the black hook shape in males is apposed exactly on the central longitudinal vein and its intersections with others along its whole course. In that sense, this study provide proof that the major pattern changes between individuals of this population are due to the variations in amount of pigment synthesized that fills the pre-set lines of the pattern displaced along the veins path. The mode of pattern expansion can be easily followed through the almost continuous trait's variation.

To summarize, the intraspecific variation in forewing pattern caught in *A. plantaginis*, a continuous expansion of shapes boundaries from a banded pattern, can be found in many other Arctiinae species (e.g., *Arctia caja*; *Haploa confusa*; *Apantesis nais*; *Eucharia festiva* (in Figure 1 of Gawne & Nijhout, 2020)). Quantitative modulation of pigment synthesis in evolution of developmental pathways is easier to achieve than rearrangement of deposition spots' location and there are numerous examples in the literature, from Arctiinae to Heliconius (Bainbridge et al., 2020; Gawne & Nijhout, 2019). For this reason, it is the most likely explanation when pattern shape variability is spotted within a sympatric group of individuals of the same species (leaving out case limit, e.g., ring species). To me, the great variability in wing patterning that can be observed in *A. plantaginis, in primis,* and also in other tiger moths, makes Arctiinae clade a

precious species group to test evo-devo theories. Different degrees of intra- and inter-specific variation are ideal to study the nature of constraints in diversification of organismal body patterning and how various genetic structures and developmental mechanisms arise to bypass such constraints. I expect that an increasing number of species from the different genus of the Arctiinae superfamily will be used as study species in the attempt of understanding phenotypic diversity in visual signal ecology (e.g., aposematism, mimicry, mate choice) from an evo-devo point of view. More renown example in that sense are, for example, the Rhopalocera genus *Heliconius* (Brien et al., 2022; Joron et al., 2006) and *Papilio* (Fujiwara, 2017; Nishikawa et al., 2015).

2. Pattern Coverage and Colour Locus

The data in my possession suggest that melanin investment in wing patterning, especially of hindwings, is correlated to colour morph. The distribution of both quantitative and categorical values of HW melanization and quantitative FW melanization showed a pattern of expression correlated to the genotype at colour locus. White males present a higher average melanization than yellows, with a lower proportion of *minus* phenotypes (HW), almost absent in white morph. WW genotype is generally associated to the highest HW and FW melanization followed by Wy and yy, suggesting that in a potential colour locus epistatic effect colour alleles may have additive effect.

Selection could have favoured the evolution of genetic correlation for the two traits, where alternative phenotypic configurations for hindwings colour and melanization occupy distinct, yet comparable, fitness peaks. In that sense, the balance of benefits and costs in expressing lower wing melanism may be more advantageous for one colour morph than to the other in specific conditions, depending on the local biotic and abiotic ecological factors. For example, in Finnish cold environment, lower black coverage could severely influence individual flying capability and general thermoregulation, however the costs are expected to be higher for whites, since yellows can resort to a higher heat absorption through the darker background colour. The possibility of allocating less energy for melanin synthesis would give yellow morph an advantage.

The results about familiar distribution highlighted two key aspects of the melanization phenotype: the genetic bases of the correlation between melanization and colour locus (e.g., epistatic effect), although present, are not simple, and not ruled by complete dominance, since families of the same genotype showed significant differences in means. Furthermore, the extremely spread distribution of some families, in contrast with packed offspring distribution of others, suggests a complex genetic bases for the trait, in which colour locus exert only a relative influence on melanization trait. Judging from differences between families of the same genotype, increasing the number of families is a priority, even at the cost of

reducing the number of individuals per family. Considering that the constant rearing environment conditions limited the role of plasticity component of variance, wing melanization variability of the sample is likely to be the effect of additive and not additive interaction of numerous loci, confirming previous hypothesis.

Sire-offspring regression

Parent-offspring regression analyses resulted in extremely high broad-sense heritability estimates for both wings, with HW value exceeding 1, showing that some conditions biased the heritability estimation. There are different aspects that could have biased the analysis, but in our case the presence of inbreeding could have been a determinant factor in heightening the estimation. In shorter timescales, heritability estimate can also be inflated due to a greater than expected relatedness between individuals included in the study. The last scenario, where parentals are more related than assumed, could have been caused by limited choice in designing our mating, that led to union of individuals from related families, since the number of captive families is always limited. It should also be considered that the common environment set by fixed rearing conditions can contribute to the parent-offspring covariance in the trait, reason why these heritability estimates have to be contextualized to these rearing conditions. Another limitation in this analysis, was represented by the use of the sole male lineage, where if present, as sex-linkage, could have inflated the estimates as well (Houde, 1992). Future studies should include female lineage as well.
All in all, there are multiple factors that could have conjunctively biased the heritability estimates from the parent-offspring analysis toward unacceptable values, hampering any strong conclusion on genetic bases of that trait variability.

It should not be forgotten that differently from what expected from stock population, heterogeneity of early life environment in the wild could significantly contribute to increase the melanization polyphenism with respect to the studied population. Further investigation on trait's plasticity should be done in the future, to assess the boundaries of environmental plasticity on the trait wing melanization. For example, a recent investigation revealed a linear effect of diet protein content on male's forewing melanization (Lindstedt et al., 2020). On contrary, another study did not find any influence of rearing temperature on wing melanization expression, although adult body and larvae's signal size shown plasticity in expression (Galarza et al., 2019). There are a couple of reasons why humidity should be tested next: humidity factor is known to be strictly connected to melanin expression adaptations, first of all for the theoretical reasons stated by the Gloger's rule (i.e., more melanised caterpillars are more protected from bacteria whose growth is enhanced by higher humidity), but also because of some experimental findings on other Lepidoptera (Hussain et al., 2011). Furthermore, looking at our stock rearing conditions, humidity could have what it takes to be a variable factor between individual boxes, determining differential rearing

conditions for full siblings: humidity inside each box is thought to be easily altered by factors out of our focus at the moment, as the quantity of food that is given but not eaten overnight, or the sunrays that can hit differentially, increasing evaporation in some boxes. All these considerations make a future study on rearing environment humidity effects a top priority for the sake of a responsible stock rearing and a better knowledge of the system.

Pedigree analysis

It is noticeable that the quantitative (pattern area) and categorical (*plus*/*minus* frequency) values in this sample are concordant with long-term pedigree data, based on the *plus*-*minus* categorical distinction, that showed a higher proportion of *minus* with yellow phenotype.
When I compared *minus* frequency between the pedigree and my sample, I initially found that the group of white specimens analysed in this study abruptly deviate from what recorded in the overall 9 years-, 24 generations-long pedigree. In specific, *minus* phenotype in white males is expected, by pedigree, to be more frequent than what shown in the sample used. Further analysis revealed that this deviation is due to a consistent decrease in *minus* white individuals within the laboratory stock across the years. What is more, when phenotypic data from the right previous generation, first of 2021 (FI21), were taken alone, proportion of white *minus* resemble almost exactly the proportion in this study, while yellow ones match it perfectly. This observation proves the adequacy of the chosen pool of families and individuals, potentially showing a good representativeness of melanization phenotype categories in the whole generation, even with this low number of families.

This initial analysis on the pedigree brought new insights of trait's segregation in the stock, where there is a consistent trend of reduction in white *minus* individuals across generations, while yellows did not show such unilateral trend. These kind of trans-generational changes in melanization classes' frequency have already been documented in wild populations, both at populational level and within each colour morphs (Galarza et al., 2014). Nevertheless, the variation spotted in the pedigree resemble more the action of a directional selective factor over time. What is more important, it seems that white *minus* phenotype (male) is increasing in frequency in the wild (personal communication by Mappes J.), further increasing the spread between the stock and the true object of investigation, the wild population. The scenario of artificial selection should be considered since the trait already appeared to be heritable (Nokelainen et al., 2013) and parent-offspring regression in this sample highlighted that less melanized fathers (HW melanization) gave birth to less melanized sons and vice versa, supporting the previous findings. It is relevant that other authors had success in artificially selecting bolder phenotypes in a similar moth (*U. ornatrix*), in just four generations (Gawne & Nijhout, 2019). The study revealed that the venous striping could be

intensified through the application of directional selective pressure. In light of our observation, the fact that details such as venous striping and pigment synthesis can be upregulated in this way leads to the question: are we inadvertently selecting for *plus* through captive rearing conditions?
A potential scenario of biased transmission of genetic variability is that more melanized white males have somewhat a faster grow rate, if not an increased survival rate, that was not possible to spot yet. In that case they would be the ones mostly used for mating (funders of the new generation), with no use for *minus* individuals from the same families that comes later on. A broader explanation is that the constant conditions and the absence of predation and sexual selection favours the more melanized white phenotype, nullifying some kind of balancing selection in the wild. Likewise, also some specific conditions of the captive rearing, as high individuals' density, could particularly benefit the *plus* white morph over the *minus* white in the race to mating. A hypothetical realistic scenario is a heightened risk of pathogen infection against which more melanized individuals are better defended (by Gloger rule). More melanized individuals could also be just more competitive and benefit from confronting the less melanized ones at higher population densities (Roulin, 2014).

These findings should remind us that, although it is fundamental to assess the phenotypic profile of stock populations since most experiments are focused on these individuals, a comparison with wild populations is needed. Determining the value of the stock in explaining the natural variation is a priority, in order to find more suitable rearing conditions and get better laboratory samples.

3. Pattern Shape and Colour Locus

Although a recent work spotted differences in forewing "pattern diversity" (variation in average size of pattern elements) between the two white genotypes, in this work, I did not find any major differences forewing's pattern shape and displacement among neither colour phenotypes nor genotypes. In that sense, forewing pattern variation in this sample showed no valuable means of distinction between WW and Wy genotypes. The dimension of a coloured patch in the pattern appeared to generate some kind of distinction between the whites, however several critical aspects hamper its significance: the range of application would be very narrow, limited to low melanization; in second place the homozygotes defining the distinction all come from the same family and the patch is small and on the wing edge, where potential small alignment and cropping errors can be a significant issue; above that, it is extremely unlikely that this variation can be spotted by eyes in an efficient manner.
From study on hindwing in this sample, I obtained promising results for white genotypes discrimination that were not spotted before (e.g., in Nokelainen et al. 2022, where pattern was treated in a more general way). Investigation on pattern

shape variation in the hindwing allowed to spot putative areas of interest for white genotypes by-eye discrimination at high levels of overall melanization. In particular, while black pigment quantity did not show any use for genotype discrimination, it appeared that the two genotypes differ in extension of specific pattern shapes. My results enlightened two slightly different mode of pattern expansion at melanization increase that could be used to distinguish between the two: WW individuals usually show hindwings with higher melanization above the hook, at the expenses of the hook boldness and the stripe below; Wy genotype show opposite trend, with less melanization above the hook with respect to the deposition in the below area. The aforementioned discriminant is indeed bounded to highly melanized individuals, where extension of the patches can be compared by eye. Its use remains doubtful at low levels of "plus" melanization since the area above the hook is never melanized and differences minimal in hook and below area. Moreover, at low melanization levels, within the *plus* interval, white genotypes are mixing again, and distinction cannot be done.

Noticeably, AHM can become completely ineffective if the population shows only mid-melanized *plus* individuals. Although unexpected, that could be a possible outcome in the last generation FI22.2, whose founders did not show any sire with AHM (personal observation), further evidencing the limited use of the aforementioned discriminant. Moreover, in the generation studied, there were only few Wy individuals at high melanization, where a proper comparison WW-Wy appeared efficient, nevertheless they all presented the same trend of enlargement of hook shape. It is hard to see the use of a discrimination method that could only be used on a small part of the sample; however, it can be valuable to study the pattern characteristics together with previously spotted salient traits. Distinction between white genotypes require multicomponent analysis, but before using UV reflectance (time consuming multispectral image analysis), linear morphometric measures, can be employed alongside with melanization information (i.e., forewing to abdomen area ratio and thorax to abdomen ratio (Nokelainen et al., 2022)).
All in all, while the covariation of some melanization differences is still unclear, it may be possible to use melanization and wing/body morphometrics in combination to predict genotypes of wild caught individuals.

If we consider the PCA space, aside from genotype discrimination purposes, the minor variations in pattern elements' shape found both in FW (proximal zone background patch) and HW (AHM to hook boldness comparison) are thought to not be enough to determine relevant fitness changes between the two distinct white genotypes. Forby once assessed the high correlation between PC1 and melanization, the overall pattern coverage was the only variable employed to test for potential fitness trade-off evolved between genotypes.

4. *Plus*/Minus Categorical Classification

Overall, the binary classification of hindwing melanization phenotypes was proven to be efficient in distinguishing 2 groups of individuals based on overall investment in pigment production, calculated as average melanization between the two wing types (Fig. 12). The actual difference is determined by HW melanization because FW melanization of *minus* individuals in many cases is indistinguishable from the one shown by many *plus* specimens. In terms of total pattern coverage, the spread between the two groups is significant and the ranges are not overlapping. The separation is mostly generated by the rarefaction of individuals at intermediate HW melanization values (between *minus* and *plus*). Although it can be expected that with an increased sampling effort the spot would get filled, it is interesting to see as intermediate values are rarer (from 30 to 40 per cent HW melanization).
In that sense, this could also suggest the presence of potential constraints to expression or development of that level of melanization. That can happen either through selection of some regulatory mechanisms that result in a rarer expression of the intermediate phenotype (i.e. inversions, or supergenes (Nishikawa et al., 2015)), or stronger selection in early life stages on individuals that would express that trait in adulthood (i.e. maladaptive juveniles (Herrel et al., 2016)). As it has been reported in previous studies, more melanized wings have their warning signal more or less hindered (Hegna et al., 2013); moreover, melanin production can negatively affect also secondary (chemical) defence intensity (Ottocento et al., 2022). Following the idea by which more than one optimum can be possible, there could be an advantage in having either highly melanized wings, to increase consistently thermoregulation efficiency, or having the minimal melanization, decreasing energy expenditure and being better protected (better defences). The intermediate state in this population could result maladapted and generate divergent selection toward either one or the other peak, with specific intermediate genetic configurations selected against.

The value of a finer wing melanism categorization based on HW was partially proven by the extent of variation entailed in the too general “plus phenotype”. Although some evident shape changes in AHM appeared to follow the melanization gradient, what I previously described as “second pattern shift” cannot be employed out of the box; its translation in a reliable discriminant would require further testing. The minor difference in black scales displacement between WW and Wy (AHM), can cause errors in allocation of intermediate phenotypes based on the aforementioned discriminator, just when AHM starts to appear.
To sum up, even assuming that a second threshold could be useful in categorization of individual overall wing melanization, assignation based on hindwing melanization could present some issues. The first is practical, it refers to the actual capability of efficient distinction between different adjacent sub-types of *plus* phenotypes based on the AHM in hindwings. Not only because

melanization grows as a continuous character in that section of the distribution, but also because of the aforementioned differences between WW and Wy. The second is more methodological, it is not given that a discrimination based on hindwing melanic coverage actually reflects overall wing melanin synthesis, as instead has been already proven true for low melanization levels. Distinction of more than two hindwings melanization groups would make no sense, if it does not directly correlate to overall melanin investment differences.

In future studies, after ascertaining the mode of covariation between AHM and overall melanization, it would be extremely valuable to perform an experiment to evaluate discriminability of different melanization classes to prove actual usability. A similar test was already carried out for this moth colour genotype discrimination, opposing human perception to computer algorithm (Nokelainen et al., 2022). In the aforementioned study, computer algorithm was trained with multispectral image values and whole body morphometrics, that could not be accurately assessed by human observers. Checking both software and human potential is the only thing that could confirm or reject the effective employability of a third class – "*plus plus*" or "*hyper-melanized*" – on parallel with phenotype-genotype association.

5. Patternize & Recolorize in Wing Pattern Analysis

After employing Recolorize and Patternize packages in a customized way, I got some information of the packages' potential and usability for our purposes. The pattern analysis workflow based on Recolorize and Patternize suggested by the developers (Weller et al., 2022) resulted in a perfect tool for precise and semi-automated quantification of melanic pattern variation in this species. Smart tools for rapid verification of automated steps and great customizability of the method are the strong points of this pattern analysis workflow. In that sense, although mostly automated, the method allows the user's intervention at almost any stage, to shape the most relevant analysis based on his specific evolutionary questions and avoid systematic errors.

The first section of the analysis (Alignment – Pixel colour binning – Area calculation) will be a great asset in future quantitative trait analysis on melanization, as a mean of rapid, dependable, and repeatable pattern coverage quantification. One specification is required, the built-in function of Patternize for automated area calculation – *patArea()* – is not appliable on the "recolorize object" (output of *recolorize2()* function). If pattern coverage quantification is the sole aim of the analysis (e.g., in a QTL analysis), pattern coverage at this point could be calculated by dividing the number of black pixels on the total number of pixel present in the area of interest (these data are stored in the "recolorize object").

Pattern PCA by Patternize is dependable and repeatable on the exact same sample, but PC values changes as soon as we change the sample, even by removing just one individual. When variability in the sample changes, the software generates new principal components to describe the variability in the dataset.
This goes by definition of PCA, and I believe it could be a great limitation to the employment of this pattern analysis in phenotyping. When we think about discrimination of phenotypic classes based on pattern differences caught by PCs, we should consider that PCs values coming from different sample pools are incomparable, since linked to each dataset composition. In addition to that, from what I could observe, the method is sensible to heterogeneous samples, because descriptors will be based on all individuals the representation of shape variance will lack the precision on close resembling individuals of interest. That can be seen in the comparison between the two PCA that were run on HW, where I had to reduce the sample to the sub-group of interest to increase the sensitivity to differences within the greatly variable *plus* group. Without that subdivision, I would not have been able to clearly extract relevant pattern descriptors as hook boldness and AHM proportion.

A strong point of Patternize is the visualization of the variance/covariance matrix of pattern boundaries in figures next to the axis, highlighting the changes caught by the PCs. That function results in a powerful tool for spotting potential macroscopic biases in pattern variation considered in the PCA and also allow to evaluate how different pattern elements differentiate the sample. This function inside *patPCA()* and the chance to check the pixel colour binning makes up for a critical aspect of the analysis, that is the alignment by landmarking. The issue regards the human ability to landmark consistently and precisely throughout the sample without introducing systematic errors. One example of that is in the first FW PCA plot in which PC2 showed a particular and unexpected pattern shift, and only after reviewing the aligned images I could recognise a recurrent error in landmarks positioning. Thanks to Patternize toolbox, I solved the issue skipping the biased PC and plotting the PC3, to get insights of presumably true pattern variation.

Overall, the procedure is suitable for distinction of pattern shapes within one single dataset, with the due precautions, but PC values themselves too sample-dependant to make pattern phenotype comparisons outside of the single analysis. One partial solution is to add the new individuals for evaluation to a standard benchmarked group of individuals taken as reference, so that PCs' distributions could remain similar, with the new samples taking their place in the almost same PCA environment. This method requires further testing, my trial with parental HW added to the sample gave promising results, but FW showed screwed distribution along a PC, without reasonable variation in that, resembling the presence of some bias or artifact.

CONCLUSIONS

The results on pattern shape variation between individuals did not lead to the discovery of effective elements for discrimination between phenotypes and color genotypes, but only some limited divergence between the two white genotypes, not enough to allow distinction. The classification into two categories of melanic phenotypes is the safest and most significant. Although the addition of a third class, splitting the *plus* class, could result more descriptive (equalizing the variability range within each class) it was not possible to define, or test clear-cut criteria for its distinction by eye. Subtle variations in pattern shape prevent hindwing melanization from being used for this purpose. The extension of black pattern on the wings appeared as a continuous character (although some values are rarer), plausibly multigenic, and correlated to colour locus expression to a certain extent; without genetic data it is impossible to test the involvement of linkage disequilibrium and epistasis, candidates to produce the observed covariation.

Given its partial covariation with the hindwing colour, it can be hypothesized a possible role for wing melanization variability in the evolution and maintenance of colour polymorphism: it is possible that a partially different "melanization strategies" between colour morphs, as showed in laboratory reared population, generates fitness differences that add up to the complex selective landscape of polymorphic aposematism. This hypothesis would require, in the future, expensive and time-consuming predation and behavioural assays and intensified wild sampling to be tested. Furthermore, I would say that it is a top priority to firstly gain more extensive information from captive population to confirm the findings from this study before starting to explore the wild one. In addition to repeating the analyzes of this study on a different and larger sample (increasing the number of families), some deeper studies on the traits plasticity are necessary to increase our knowledge of the trait and to give more credit to the results of this study. Phenotypic plasticity of melanization and LHT remain untested for some environmental factors, with the risk of confusing estimates of heritability and misjudging phenotypic distributions. First to be tested should be environmental humidity, on which there are no data on *A. plantaginis* in the literature and because water supply is reported to be a critical aspect of early life resource environment.

It is extremely important in future studies to investigate in more detail the proportions of the different colour-melanism configurations in the wild, to get real information on the variety selected in the wild. What is more, the temperature rise from the climate change could be shifting the balances, as it is suggested by the higher proportion of white *minus* in the recent years (personal communication by Johanna Mappes). In a warming up boreal climate region, the monitoring of phenotypes related to heat absorption in polymorphic systems, as the wood tiger moth, could be a precious source of data on climate change effects on biodiversity

in animal communities in a generational timescale. Thanks to its extended polymorphism and short lifecycle, this moth has a great potential as bioindicator. One key feature in the upcoming research on melanization will be certainly represented by the QTL analysis that could be greatly enhanced by the use of a Patternize/Recolorize workflow, in attempt to address questions about the genetic bases of the trait.

BIBLIOGRAPHY

Adams, W. J., Graf, E. W., & Anderson, M. (2019). Disruptive coloration and binocular disparity: Breaking camouflage. *Proceedings of the Royal Society B: Biological Sciences*, *286*(1896). https://doi.org/10.1098/rspb.2018.2045

Badejo, O., Skaldina, O., & Sorvari, J. (2018). Spatial and Temporal Variation in Thermal Melanism in the Aposematic Common Wasp (Vespula vulgaris) in Northern Europe. *Annales Zoologici Fennici*, *55*(1–3), 67–78. https://doi.org/10.5735/086.055.0107

Bainbridge, H. E., Brien, M. N., Morochz, C., Salazar, P. A., Rastas, P., & Nadeau, N. J. (2020). Limited genetic parallels underlie convergent evolution of quantitative pattern variation in mimetic butterflies. *Journal of Evolutionary Biology*, *33*(11), 1516–1529. https://doi.org/10.1111/jeb.13704

Belleghem, S. M. Van, Papa, R., Ortiz-zuazaga, H., Jiggins, C. D., Mcmillan, W. O., Counterman, B. A., Kingdom, U., Rico, P., Campus, R. P., Rico, P., Juan, S., Campus, R. P., Rico, P., & Unit, E. (2019). *HHS Public Access*. *2018*(2), 390–398. https://doi.org/10.1111/2041-210X.12853.patternize

BRAKEFIELD, P. M., & LIEBERT, T. G. (1985). Studies of colour polymorphism in some marginal populations of the aposematic jersey tiger moth Callimorpha quadripunctaria. *Biological Journal of the Linnean Society*, *26*(3), 225–241. https://doi.org/10.1111/j.1095-8312.1985.tb01634.x

Brien, M. N., Enciso-Romero, J., Lloyd, V. J., Curran, E. V, Parnell, A. J., Morochz, C., Salazar, P. A., Rastas, P., Zinn, T., & Nadeau, N. J. (2022). The genetic basis of structural colour variation in mimetic Heliconius butterflies. *Philosophical Transactions of the Royal Society B: Biological Sciences*, *377*(1855), 20200505. https://doi.org/10.1098/rstb.2020.0505

Briolat, E. S., Burdfield-Steel, E. R., Paul, S. C., Rönkä, K. H., Seymoure, B. M., Stankowich, T., & Stuckert, A. M. M. (2019). Diversity in warning coloration: selective paradox or the norm? *Biological Reviews*, *94*(2), 388–414. https://doi.org/https://doi.org/10.1111/brv.12460

Clusella-Trullas, S., Terblanche, J. S., Blackburn, T. M., & Chown, S. L. (2008). Testing the thermal melanism hypothesis: A macrophysiological approach. *Functional Ecology*, *22*(2), 232–238. https://doi.org/10.1111/j.1365-2435.2007.01377.x

Cott, H. B. (1940). Adaptive coloration in animals. In *Adaptive coloration in animals.* Oxford.

Cuthill, I. C., Allen, W. L., Arbuckle, K., Caspers, B., Chaplin, G., Hauber, M. E., Hill, G. E., Jablonski, N. G., Jiggins, C. D., Kelber, A., Mappes, J., Marshall, J., Merrill, R., Osorio, D., Prum, R., Roberts, N. W., Roulin, A., Rowland, H. M., Sherratt, T. N., … Caro, T. (2017). The biology of color. *Science*, *357*(6350). https://doi.org/10.1126/science.aan0221

Das, S., Hirano, M., Tako, R., McCallister, C., & Nikolaidis, N. (2012). Evolutionary

genomics of immunoglobulin-encoding Loci in vertebrates. *Current Genomics*, *13*(2), 95–102. https://doi.org/10.2174/138920212799860652

De Pasqual, C., Suisto, K., Kirvesoja, J., Gordon, S., Ketola, T., & Mappes, J. (2022). Heterozygote advantage and pleiotropy contribute to intraspecific color trait variability. *Evolution*, 1–15. https://doi.org/10.1111/evo.14597

Doktorovová, L., Exnerová, A., Hotová Svádová, K., Štys, P., Adamová-Ježová, D., Zverev, V., Kozlov, M. V., & Zvereva, E. L. (2019). Differential Bird Responses to Colour Morphs of an Aposematic Leaf Beetle may Affect Variation in Morph Frequencies in Polymorphic Prey Populations. *Evolutionary Biology*, *46*(1), 35–46. https://doi.org/10.1007/s11692-018-9465-8

Drinkwater, E., Allen, W. L., Endler, J. A., Hanlon, R. T., Holmes, G., Homziak, N. T., Kang, C., Leavell, B. C., Lehtonen, J., Loeffler-Henry, K., Ratcliffe, J. M., Rowe, C., Ruxton, G. D., Sherratt, T. N., Skelhorn, J., Skojec, C., Smart, H. R., White, T. E., Yack, J. E., … Umbers, K. D. L. (2022). A synthesis of deimatic behaviour. *Biological Reviews*, *97*(6), 2237–2267. https://doi.org/10.1111/brv.12891

Fujiwara, H. (2017). Molecular Mechanism and Evolutionary Process Underlying Female-Limited Batesian Mimicry in Papilio polytes. In *Diversity and Evolution of Butterfly Wing Patterns: An Integrative Approach* (pp. 189–201). https://doi.org/10.1007/978-981-10-4956-9

Galarza, J. A., Dhaygude, K., Ghaedi, B., Suisto, K., Valkonen, J., & Mappes, J. (2019). Evaluating responses to temperature during pre-metamorphosis and carry-over effects at post-metamorphosis in the wood tiger moth (Arctia plantaginis). *Philosophical Transactions of the Royal Society B: Biological Sciences*, *374*(1783). https://doi.org/10.1098/rstb.2019.0295

Galarza, J. A., Nokelainen, O., Ashrafi, R., Hegna, R. H., & Mappes, J. (2014). Temporal relationship between genetic and warning signal variation in the aposematic wood tiger moth (Parasemia plantaginis). *Molecular Ecology*, *23*(20), 4939–4957. https://doi.org/10.1111/mec.12913

Gawne, R., & Nijhout, H. F. (2019). Expanding the nymphalid groundplan's domain of applicability: Pattern homologies in an arctiid moth (Utetheisa ornatrix). *Biological Journal of the Linnean Society*, *126*(4), 912–924. https://doi.org/10.1093/biolinnean/bly193

Gawne, R., & Nijhout, H. F. (2020). *The Arctiid Archetype : A New Lepidopteran Groundplan*. *8*(June), 1–12. https://doi.org/10.3389/fevo.2020.00175

Gordon, S. P., Kokko, H., Rojas, B., Nokelainen, O., & Mappes, J. (2015). Colour polymorphism torn apart by opposing positive frequency-dependent selection, yet maintained in space. *Journal of Animal Ecology*, *84*(6), 1555–1564. https://doi.org/10.1111/1365-2656.12416

Hegna, R. H., & Mappes, J. (2014). Influences of geographic differentiation in the forewing warning signal of the wood tiger moth in Alaska. *Evolutionary Ecology*, *28*(6), 1003–1017. https://doi.org/10.1007/s10682-014-9734-7

Hegna, R. H., Nokelainen, O., Hegna, J. R., & Mappes, J. (2013). To quiver or to

shiver: Increased melanization benefits thermoregulation, but reduces warning signal efficacy in the wood tiger moth. *Proceedings of the Royal Society B: Biological Sciences*, *280*(1755). https://doi.org/10.1098/rspb.2012.2812

Henze, M. J., Lind, O., Mappes, J., Rojas, B., & Kelber, A. (2018). An aposematic colour-polymorphic moth seen through the eyes of conspecifics and predators – Sensitivity and colour discrimination in a tiger moth. *Functional Ecology*, *32*(7), 1797–1809. https://doi.org/10.1111/1365-2435.13100

Herrel, A., Lopez-Darias, M., Vanhooydonck, B., Cornette, R., Kohlsdorf, T., & Brandt, R. (2016). Do Adult Phenotypes Reflect Selection on Juvenile Performance? A Comparative Study on Performance and Morphology in Lizards. *Integrative and Comparative Biology*, *56*(3), 469–478. https://doi.org/10.1093/icb/icw010

Holmes, G. G., Delferrière, E., Rowe, C., Troscianko, J., & Skelhorn, J. (2018). Testing the feasibility of the startle-first route to deimatism. *Scientific Reports*, *8*(1), 1–8. https://doi.org/10.1038/s41598-018-28565-w

Honma, A., Mappes, J., & Valkonen, J. K. (2015). Warning coloration can be disruptive: Aposematic marginal wing patterning in the wood tiger moth. *Ecology and Evolution*, *5*(21), 4863–4874. https://doi.org/10.1002/ece3.1736

Houde, A. E. (1992). Sex-linked heritability of a sexually selected character in a natural population of Poecilia reticulata (Pisces: Poeciliidae) (guppies). *Heredity*, *69*(3), 229–235. https://doi.org/10.1038/hdy.1992.120

Hussain, M., Khan, S., Naeem, M., & Nasir, M. (2011). Effect of Rearing Temperature and Humidity on Fecundity and Fertility of Silkworm, Bombyx mori L. (Lepidoptera: Bombycidae). *Pakistan Journal of Zoology*, *43*, 979–985.

Idris, E. (2013). Aposematic polymorphism in the tropical butterfly Danaus chrysippus: A review. *Egyptian Academic Journal of Biological Sciences. A, Entomology*, *6*(1), 67–78. https://doi.org/10.21608/eajbsa.2013.13820

Jablonski, N. G., & Chaplin, G. (2000). The evolution of human skin coloration. *Journal of Human Evolution*, *39*(1), 57–106. https://doi.org/https://doi.org/10.1006/jhev.2000.0403

Joron, M., Jiggins, C. D., Papanicolaou, A., & McMillan, W. O. (2006). Heliconius wing patterns: an evo-devo model for understanding phenotypic diversity. *Heredity*, *97*(3), 157–167. https://doi.org/10.1038/sj.hdy.6800873

Joron, M., & Mallet, J. L. B. (1998). Diversity in mimicry: Paradox or paradigm? *Trends in Ecology and Evolution*, *13*(11), 461–466. https://doi.org/10.1016/S0169-5347(98)01483-9

Karell, P., Ahola, K., Karstinen, T., Valkama, J., & Brommer, J. E. (2011). Climate change drives microevolution in a wild bird. *Nature Communications*, *2*(1), 208. https://doi.org/10.1038/ncomms1213

Kingsolver, J. G. (1987). Predation, thermoregulation, and wing color in pierid

butterflies. *Oecologia*, *73*(2), 301–306. https://doi.org/10.1007/BF00377522

Kozlov, M. V, Oudendijk, Z., Forsman, A., Lanta, V., Barclay, M. V. L., Gusarov, V. I., Gustafsson, B., Huang, Z.-Z., Kruglova, O. Y., Marusik, Y. M., Mikhailov, Y. E., Mutanen, M., Schneider, A., Sekerka, L., Sergeev, M. E., Zverev, V., & Zvereva, E. L. (2022). Climate shapes the spatiotemporal variation in color morph diversity and composition across the distribution range of Chrysomela lapponica leaf beetle. *Insect Science*, *29*(3), 942–955. https://doi.org/https://doi.org/10.1111/1744-7917.12966

Kuwalekar, M., Deshmukh, R., Padvi, A., Kunte, K., & Martin, S. (2020). *Molecular Evolution and Developmental Expression of Melanin Pathway Genes in Lepidoptera*. *8*(July), 1–10. https://doi.org/10.3389/fevo.2020.00226

Lindstedt, C., Schroderus, E., Lindström, L., Mappes, T., & Mappes, J. (2016). Evolutionary constraints of warning signals: A genetic trade-off between the efficacy of larval and adult warning coloration can maintain variation in signal expression. *Evolution*, *70*(11), 2562–2572. https://doi.org/10.1111/evo.13066

Lindstedt, C., Suisto, K., & Mappes, J. (2020). Appearance before performance? Nutritional constraints on life-history traits, but not warning signal expression in aposematic moths. *Journal of Animal Ecology*, *89*(2), 494–505. https://doi.org/10.1111/1365-2656.13103

Lynch, M., & Walsh, B. (1998). *Genetics and analysis of quantitative traits* (Vol. 1). Sinauer Sunderland, MA.

Majerus, M. E. N. (1998). Melanism. *Evolution in Action*.

Martínez-Freiría, F., Pérez i de Lanuza, G., Pimenta, A. A., Pinto, T., & Santos, X. (2017). Aposematism and crypsis are not enough to explain dorsal polymorphism in the Iberian adder. *Acta Oecologica*, *85*, 165–173. https://doi.org/https://doi.org/10.1016/j.actao.2017.11.003

Mazo-Vargas, A., Concha, C., Livraghi, L., Massardo, D., Wallbank, R. W. R., Zhang, L., Papador, J. D., Martinez-Najera, D., Jiggins, C. D., & Kronforst, M. R. (2017). Macroevolutionary shifts of WntA function potentiate butterfly wing-pattern diversity. *Proceedings of the National Academy of Sciences*, *114*(40), 10701–10706.

Mochida, K. (2011). Combination of local selection pressures drives diversity in aposematic signals. *Evolutionary Ecology*, *25*(5), 1017–1028. https://doi.org/10.1007/s10682-011-9471-0

Monteiro, A. (2008). Alternative models for the evolution of eyespots and of serial homology on lepidopteran wings. *Bioessays*, *30*(4), 358–366.

Nijhout, H. F. (1991). *The development and evolution of butterfly wing patterns*. Smithsonian Institution.

NIJHOUT, H. F., & WRAY, G. A. (1988). Homologies in the colour patterns of the genus Heliconius (Lepidoptera: Nymphalidae). *Biological Journal of the*

Linnean Society, *33*(4), 345–365.

Nishikawa, H., Iijima, T., Kajitani, R., Yamaguchi, J., Ando, T., Suzuki, Y., Sugano, S., Fujiyama, A., Kosugi, S., Hirakawa, H., Tabata, S., Ozaki, K., Morimoto, H., Ihara, K., Obara, M., Hori, H., Itoh, T., & Fujiwara, H. (2015). A genetic mechanism for female-limited Batesian mimicry in Papilio butterfly. *Nature Genetics*, *47*(4), 405–409. https://doi.org/10.1038/ng.3241

Nokelainen, O., Galarza, J. A., Kirvesoja, J., Suisto, K., & Mappes, J. (2022). Genetic colour variation visible for predators and conspecifics is concealed from humans in a polymorphic moth. *Journal of Evolutionary Biology*, *35*(3), 467–478. https://doi.org/10.1111/jeb.13994

Nokelainen, O., Hegna, R. H., Reudler, J. H., Lindstedt, C., & Mappes, J. (2012). Trade-off between warning signal efficacy and mating success in the wood tiger moth. *Proceedings of the Royal Society B: Biological Sciences*, *279*(1727), 257–265. https://doi.org/10.1098/rspb.2011.0880

Nokelainen, O., Lindstedt, C., & Mappes, J. (2013). Environment-mediated morph-linked immune and life-history responses in the aposematic wood tiger moth. *Journal of Animal Ecology*, *82*(3), 653–662. https://doi.org/10.1111/1365-2656.12037

Noonan, B. P., & Comeault, A. A. (2009). The role of predator selection on polymorphic aposematic poison frogs. *Biology Letters*, *5*(1), 51–54. https://doi.org/10.1098/rsbl.2008.0586

Ojala, K., Lindström, L., & Mappes, J. (2007). Life-history constraints and warning signal expression in an arctiid moth. *Functional Ecology*, *21*(6), 1162–1167. https://doi.org/10.1111/j.1365-2435.2007.01322.x

Ottocento, C., Rojas, B., Burdfield-steel, E., & Furlanetto, M. (2022). *Differential resource allocation between melanin-based colour morphs in an aposematic moth*.

Pasqual, C. De, Selenius, E., Burdfield-steel, E., & Mappes, J. (2022). *Genetic background and antennae variation affect pheromone signaling and male recruitment in a moth species*.

Rojas, B., Burdfield-Steel, E., De Pasqual, C., Gordon, S., Hernández, L., Mappes, J., Nokelainen, O., Rönkä, K., & Lindstedt, C. (2018). Multimodal aposematic signals and their emerging role in mate attraction. *Frontiers in Ecology and Evolution*, *6*(JUL). https://doi.org/10.3389/fevo.2018.00093

Rojas, B., Valkonen, J., & Nokelainen, O. (2015). Aposematism. *Current Biology*, *25*(9), R350–R351. https://doi.org/10.1016/j.cub.2015.02.015

Rönkä, K., Valkonen, J. K., Nokelainen, O., Rojas, B., Gordon, S., Burdfield-Steel, E., & Mappes, J. (2020). Geographic mosaic of selection by avian predators on hindwing warning colour in a polymorphic aposematic moth. *Ecology Letters*, *23*(11), 1654–1663. https://doi.org/10.1111/ele.13597

Roulin, A. (2014). Melanin-based colour polymorphism responding to climate

change. *Global Change Biology*, *20*(11), 3344–3350. https://doi.org/10.1111/gcb.12594

Ruxton, G. D., Sherratt, T. N., & Speed, M. P. (2004). *Avoiding Attack: The Evolutionary Ecology of Crypsis, Warning Signals and Mimicry*. Oxford University Press. https://doi.org/10.1093/acprof:oso/9780198528609.001.0001

Schlenoff, D. H. (1985). The startle responses of blue jays to Catocala (Lepidoptera: Noctuidae) prey models. *Animal Behaviour*, *33*(4), 1057–1067.

Speed, M. P., & Ruxton, G. D. (2007). How bright and how nasty: Explaining diversity in warning signal strength. *Evolution*, *61*(3), 623–635. https://doi.org/10.1111/j.1558-5646.2007.00054.x

Sugumaran, M. (2002). Comparative biochemistry of eumelanogenesis and the protective roles of phenoloxidase and melanin in insects. *Pigment Cell Research*, *15*(1), 2–9. https://doi.org/10.1034/j.1600-0749.2002.00056.x

Talloen, W., Van Dyck, H., & Lens, L. (2004). The cost of melanization: Butterfly wing coloration under environmental stress. *Evolution*, *58*(2), 360–366. https://doi.org/10.1111/j.0014-3820.2004.tb01651.x

Van Belleghem, S. M., Alicea Roman, P. A., Carbia Gutierrez, H., Counterman, B. A., & Papa, R. (2020). Perfect mimicry between Heliconius butterflies is constrained by genetics and development. *Proceedings of the Royal Society B: Biological Sciences*, *287*(1931), 20201267. https://doi.org/10.1098/rspb.2020.1267

Weller, H. I., Hiller, A. E., Lord, N. P., & Van Belleghem, S. M. (2022). Flexible color segmentation of biological images with the R package recolorize. *BioRxiv*, 2022.04.03.486906. http://biorxiv.org/content/early/2022/07/18/2022.04.03.486906.abstract

Wittkopp, P. J., Stewart, E. E., Arnold, L. L., Neidert, A. H., Haerum, B. K., Thompson, E. M., Akhras, S., Smith-Winberry, G., & Shefner, L. (2009). Intraspecific Polymorphism to Interspecific Divergence: Genetics of Pigmentation in Drosophila. *Science*, *326*(5952), 540–544. https://doi.org/10.1126/science.1176980

Yuan, M. L., Jung, C., Bell, R. C., & Nelson, J. L. (2022). Aposematic patterns shift continuously throughout the life of poison frogs. *Journal of Zoology*, *317*(4), 241–248. https://doi.org/https://doi.org/10.1111/jzo.12977

Zylinski, S., & Osorio, D. (2013). Visual contrast and color in rapid learning of novel patterns by chicks. *Journal of Experimental Biology*, *216*(22), 4184–4189. https://doi.org/10.1242/jeb.085001

APPENDIX

R script for Hindwings

Here is reported only the script used for Hindwings since Forewing analysis followed exactly the same steps.

```
############################
#Landmarks Alignment and pixel colour binning
############################
library(patternize)
library(raster)
library(RNiftyReg)

prepath<- "HW/"
#setwd("~/Melanization Analyses_def/DORS/dFW")

IDlist <- tools::file_path_sans_ext(dir("HW", ".JPG"))

imageList <- makeList(IDlist, type = "image",
                      prepath= "HW",
                      extension = ".JPG")
landmarkList <- makeList(IDlist,
                         type = "landmark",
                         prepath = prepath,
                         extension = ".txt")

target <- landmarkList[["FI21.2-43.28_dhwL"]]
mask <- read.table("HW/mask/mask43.28_dhwL.txt", header = FALSE)

par(mfrow=c(1,4))

imageList_aligned <- alignLan(imageList, landmarkList, transformRef = target,
                              res = c(240,220),
                              adjustCoords = TRUE, #if I want to obtain arrays
                              plotTransformed = F, #false it'll goes faster
                              resampleFactor = 3,
                              cartoonID = "FI21.2-43.28_dhwL",
        #NB: ERROR imageEx not found when given cartoonID is not in the image list!
                              maskOutline = mask,
                              inverse = FALSE
                              )

# save RDS file -- using png now
saveRDS(imageList_aligned, "HW/rds_files/120HW_alignJPG-43.28_rspl3_2.rds")
# read it in:
imageList_aligned <- readRDS("HW/rds_files/120HW_alignJPG-43.28_rspl3_2.rds")

#RECOLORIZE
    library(recolorize)
# 1- from raster to array
imgs <- lapply(imageList_aligned, brick_to_array)

names(imgs) <- names(imageList_aligned)
par(mar= rep(0.1,4))
par(mfrow=c(6,5)); lapply(imgs, plotImageArray)
# save raster extents for later conversion
extent_list <- lapply(imageList_aligned, extent)

#1A - Blurring
blurr_imgs<- vector("list", length= length(imgs))
names(blurr_imgs) <- names(imgs)
#par(mfrow= c(4,1))
for (i in 1:length(imgs)) {
```

```
  blurr_imgs [[i]]<- blurImage(imgs[[i]], blur_function = "blur_anisotropic",
                               amplitude = 20, sharpness=0.300, plotting=FALSE)
  print(i)
}
##blurImage functions only on arrays! so after converting bricks (raster) to arrays
##########RECOLORING
par(mfrow= c(5,8))
par(mar= rep(0.1,4))
lapply(imgs, plotImageArray)
lapply(blurr_imgs, plotImageArray)

# make an empty list for storing the recolorized objects
rc_list <- vector("list", length(imgs))
names(rc_list) <- names(imgs)

               par(mfrow=c(1,1))
# for every image, run the same recolorize2 function to fit a recolorize object:

for (i in 1:length(imgs)) {
       rc_list[[i]] <- recolorize2(imgs[[i]], bins = c(6,2,6),
                      n_final = 2,
                      plotting = TRUE)
              print(i)
}
par(mfrow=c(5,5));  for (i in 1:length(rc_list)) {
recolorize::plotImageArray(recoloredImage(rc_list[[i]]))
}

               rc_blur_list <- vector("list", length(imgs))
names(rc_blur_list) <- names(imgs)

for (i in 1:length(imgs)) {
  rc_blur_list[[i]] <- recolorize2(blurr_imgs[[i]], bins = c(5,2,5),
                         n_final = 2,
                         plotting = TRUE)
               print(i)
 }

par(mfrow=c(7,6)); for (i in 1:length(imgs)) {
                   recolorize::plotImageArray(recoloredImage(rc_blur_list[[i]]))
                    }

               rc_tresh <- vector("list", length(imgs))
               names(rc_tresh) <- names(imgs)

    for (i in 1:length(imgs)) {
  rc_tresh[[i]] <- thresholdRecolor(rc_blur_list[[i]], pct = 0.1, plotting = FALSE)
  print(i)
  }
##-TRESHOLDED RECOLORED IMAGE ARE FAR BETTER AT EDGE DISTINCTION!
#all the minor issue with single photos should be corrected one by one separately

par(mfrow=c(7,6)); for (i in 1:length(imgs)) {
                   recolorize::plotImageArray(recoloredImage(rc_tresh[[i]]))
}

#EXPORT RECOLORED IMAGES IN JPG & PNG - customed function
source("~/Melanization Analyses_def/FX/FX_export_recol_imgs.R")
expRC_JPG(rcList = rc_tresh, exp_path = "HW/rc_exp")           #recoloured JPG
source("~/Melanization Analyses_def/FX/FX_export_rc_PNG.R")
expRC_PNG(rcList = rc_tresh, exp_path = "HW/PNGs/rc_exp")      #recoloured PNG
source("~/Melanization Analyses_def/FX/FX_expPNG_imgs.R")
exp_PNG(rcList = imgs, exp_path = "HW/PNGs/aligned")        #original, aligned PNG
```

```
############################
# Pattern shape analyis
############################
library(patternize)
library(raster)

# make sure these dependencies are installed:
### ("rgdal","abind","raster","sp","RniftyReg")
library(viridis)
# List with samples
setwd("C:/Users/paolo/OneDrive/Desktop/HW")
IDlist <- tools::file_path_sans_ext(dir("rc_exp", ".JPG"))


#source("C:/Users/paolo/Documents/Melanization Analyses_def/FX/FX_rename_landmarks
files.R")
#RC_lm_listing("rc_exp", ".JPG", "rc_lm")

#lm
prepath <- 'rc_lm'
extension <- '.txt'
landmarkList <- makeList(IDlist, 'landmark', prepath, extension)

# make list with images NB: it DOESN'T WORK WITH PNGs!
prepath <- 'rc_exp'
extension <- '.JPG'
imageList <- makeList(IDlist, 'image', prepath, extension); remove(extension);
remove(prepath)

# run alignment of color patterns
RGB <- sampleRGB(imageList[[7]], resampleFactor = NULL,
                 crop = c(0,0,0,0))
RGB <- c(88, 82, 70) #Dark brown
##STACK
#for bigger analysis, it might be good to use a single target for all of your
analyses
#so they will be comparable (always aligned to same reference sample).
# For this, use 'transformRef = target'

target <- landmarkList[[5]]
rasterList_lanRGB <- patLanRGB(imageList, landmarkList, RGB, transformRef= target,
                               resampleFactor = 1,
                               ##NBBB on recolored Images the  resampling is futile,
                              # given the fact they are already at a lower resolution
                               colOffset = 0.05, res =  150,crop = TRUE,
                               adjustCoords = FALSE, plot = 'stack')

# sum the colorpatterns
summedRaster_lanRGB <- sumRaster(rasterList_lanRGB, IDlist, type = 'RGB')

# plot heatmap
cartoon <- read.table('mask/rc_mask240x230Small3.txt', h = F)
#cartoon <- read.table(file.choose(), h = F)

par(mfrow=c(1,1))
#colfunc <- c("black","lightblue","blue","green", "yellow","red")
colfunc <- inferno(100)
plotHeat(summedRaster_lanRGB, IDlist,  refShape = 'target', plotCartoon = TRUE,
       outline = cartoon,
              landList = landmarkList, adjustCoords = FALSE,
              imageList = imageList, flipRaster = "y", cartoonID = "rc_mask29.1HW",
       cartoonFill = 'black', cartoonOrder = 'under',
       colpalette = colfunc)
```

```
# Plot PCA
# Make population and color list
source("~/Melanization Analyses_def/FX/get_fam_names.R")
Family<-get_fam_names(IDlist = IDlist)
Genotype<- ifelse(Family<33, "Wy",
                  ifelse(Family==35, "yy",
                         ifelse(37<Family & Family<40, "WW",
                                ifelse(42<Family & Family<45, "WW", "yy")
                         )))
popList <- list(IDlist)
colList <- "dark blue"
##project if I have time
WW <- which(Genotype=="WW")
Wy <- which(Genotype=="Wy")
yy <- which(Genotype=="yy")
popList <- list(WW, Wy, yy)
colList <- c("red", "green", "blue")

TotalList <- rasterList_lanRGB
library(recolorize)

source("C:/Users/paolo/Documents/Melanization Analyses_def/FX/FX_imgImport.R")
images<-imgImport("rc_exp/pngs", ".png")
#ImgImport is a custom function to import images to be plotted in PCA plot

source("C:/Users/paolo/Documents/Melanization                    Analyses_def/FX/FX_my_patPCA-
plotMain_addImg.R")
## (here I call my_patPCA_addImg, customize, from patPCA(), it allows to give a plot
title and
#plot individual's images on their coordinates
pcaOut <- my_patPCA_addImg(TotalList, popList, colList, symbolList = symbolList,
                           plot = TRUE, plotType = 'points', plotChanges = TRUE,
                           PCx = 1, PCy = 2, plotCartoon = TRUE, refShape = 'target',
                           outline = cartoon, flipRaster = 'y',
                           imageList = imageList, normalized = TRUE,
                           cartoonID = 'rc_maskHW', cartoonFill = 'black',
                           cartoonOrder = 'under',
                           legendTitle = 'absent  -  PREDICTED BLACK     -     filled',
                           plot_main = "Pattern-PCA_RcHW", images = images,
                           list_length = length(images), img_size = 2)

patArea<- patArea(TotalList, IDlist= IDlist,type = 'RGB', landList = landmarkList,
refShape = "target",
                  outline = cartoon, adjustCoords = FALSE, imageList=imageList)
# it's all based on PIXELS WITHIN THE CARTOON
#pay attention at cartoon orientation and dimensions
melanization<- as.numeric(patArea$Area)

PC1<-as.array(pcaOut[[3]]$x[,1])
PC2<-as.array(pcaOut[[3]]$x[,2])

PCA_tot<- as.data.frame(cbind(PC1,PC2, "Family" = Family, "Genotype"= Genotype,
                              "Melanization"= melanization))
PCA_tot$PC1 <- as.numeric(PCA_tot$PC1)
PCA_tot$PC2 <- as.numeric(PCA_tot$PC2)
source("C:/Users/paolo/Documents/Melanization Analyses_def/FX/get_fam_names.R")
row.names(PCA_tot)<- get_fam_names(IDlist, left_sep = "[_]", right_sep = "[_]")

save(Patt_Analysis_Results, file="Pattern_Analysis_Results.csv")

library(recolorize)
PCx <- 1; PCy <- 2
pca_summary<- summary(pcaOut[[3]]$x)
limits <- apply(pcaOut[[3]]$x[ , c(PCx, PCy)], 2, range)
par(mar = c(4, 4, 3, 3))
```

```
plot(PC1, PC2,
     xlim = limits[ , 1] + c(-2, 2),
     ylim = limits[ , 2] + c(-2, 2),
     xlab=paste0('PC1 (', round(summary(pcaOut[[3]])$importance[2, PCx]*100, 1), ' %)'),
     ylab=paste0('PC2 (', round(summary(pcaOut[[3]])$importance[2, PCy]*100, 1), ' %)'),
     pch=19, cex=1.25, main= "Patternize PCA Hindwing")

for (i in 1:length(IDlist)) {
    add_image(images[[i]],
              x = PC1[[i]],
              y = PC2[[i]],
              width = 3.0)
}
par(mfrow=c(1,1))

plot(PC1, PC2, pch=19, cex=3, col= as.factor(Genotype))
title(main = "PattPCA_HW")
for (i in 1:length(imageList)) {
    text(x = PC1,
         y = PC2, labels = Family, adj = NULL,
         pos = NULL, offset = 0, cex = 0.68, col="white")
}

#OTHER PLOTS
library(ggplot2); library(ggplotAssist)

ggplot(PCA_tot, aes(x=Genotype, y=melanization))+ #aes(color=Family)
    geom_boxplot(fill=c("white", "light grey", "yellow"), width=0.3)+
    ggtitle("Melanizatio X Genotypes")

ggplot(PCA_tot, aes(x=Genotype, y=melanization, color=Family))+ #aes(color=Family)
    geom_boxplot(width=0.7)+
    ggtitle("HW Melanization variance among Families and Genotypes")

ggplot(PCA_tot, aes(x=PC1, y=melanization))+
    ggtitle("Melanizatio - PC1 correlation HW")+
    geom_point(size=1)

#################
###STATISTICAL ANALYSIS
#################
file.choose() #PA_Result_tot
summary(PA_Results_tot)
attach(PA_Results_tot)


#####Correlation HW-FW Melanization
cor_FW_HW_Mel_WW<-cor.test(W_W$HW_Melanization,W_W$FW_Melanization)
cor_FW_HW_Mel_Wy<-cor.test(W_y$HW_Melanization,W_y$FW_Melanization)
cor_FW_HW_Mel_yy<-cor.test(y_y$HW_Melanization,y_y$FW_Melanization)
cor_FW_HW_Mel_W_<-cor.test(W_$HW_Melanization,W_$FW_Melanization)

attach(PA_Results_HW)

WW<-which(PA_Results_HW$Genotype=="WW")
W_W<- PA_Results_HW[WW,]
minusWW<-which(W_W$PC1_HW>30)

yy<-which(PA_Results_HW$Genotype=="yy")
y_y<- PA_Results_HW[yy,]
minusyy<-which(y_y$PC1_HW>30)

Wy<-which(PA_Results_HW$Genotype=="Wy")
W_y<- PA_Results_HW[Wy,]
```

```
W_<- rbind.data.frame(W_W,W_y)

summary_W_<-summary(W_)
summary_WW<- summary(W_W)
summary_Wy<- summary(W_y)
summary_yy<- summary(y_y)


#CORRELATION PC1 Mel
HW_corPC1_Mel<-cor.test(PC1_HW, HW_Melanization)
HW_corPC1_Mel_WW<-cor.test(W_W$PC1_HW, W_W$HW_Melanization)
HW_corPC1_Mel_Wy<-cor.test(W_y$PC1_HW, W_y$HW_Melanization)
HW_corPC1_Mel_yy<-cor.test(y_y$PC1_HW, y_y$HW_Melanization)

HW_MelxPhen_wilcox<-wilcox.test(W_$HW_Melanization, y_y$HW_Melanization)
HW_MelxGen_wilcox<- pairwise.wilcox.test(HW_Melanization, Genotype)

corrHW_FW<-cor.test(FW_Melanization, HW_Melanization)

library(writexl)
write_xlsx(HW_Anova_tests,"C:/Users/paolo/OneDrive/Desktop/HW/results/final
results/HW_Anova_tests.xlsx")
save(HW_Anova_tests, file="C:/Users/paolo/OneDrive/Desktop/HW/results/final
results/HW_Anova_tests.Rda")
attach(PA_Results_tot)

attach(PA_Results_HW)
#testing equality of means
HW_Anova_tests<- vector("list")
HW_Anova_tests[["HWxPhen"]]<-oneway.test(HW_Melanization~Phenotype)
HW_Anova_tests[["HWxGen"]]<-oneway.test(HW_Melanization~Genotype)
HW_Anova_tests[["HWxFam"]]<-oneway.test(HW_Melanization~Family)
HW_Anova_tests[["HWxFam_W_"]]<-oneway.test(W_$HW_Melanization~W_$Family)
HW_Anova_tests[["HWxFam_WW"]]<-oneway.test(W_W$HW_Melanization~W_W$Family)
HW_Anova_tests[["HWxFam_Wy"]]<-oneway.test(W_y$HW_Melanization~W_y$Family)
HW_Anova_tests[["HWxFam_yy"]]<-oneway.test(y_y$HW_Melanization~y_y$Family)

#############
#FW-HW-Tot_Mel comparison
attach(PA_Results_tot)
for (i in 1:length(PA_Results_tot)) {
    Overall_mel[i]<-as.numeric((FW_Melanization[[i]]+ HW_Melanization[[i]])/2)
}
PA_Results_tot<- cbind.data.frame(PA_Results_tot, "Overall_mel"= Overall_mel)
Overall_melan<-order(PA_Results_tot$Overall_mel, decreasing = FALSE)
Tot_mel<- PA_Results_tot$Overall_mel[Overall_melan]

cor.test(Overall_mel,HW_Melanization)
cor.test(Overall_mel,FW_Melanization)

#PLOTTING
plot(Tot_mel, pch=19, cex=2, col= as.factor(PA_Results_tot$Genotype[Overall_melan]),
     ylim=c(min(HW_Melanization),max(FW_Melanization)),
     ylab= "Pattern coverage", xlab="Individual_n°")
##### HW
points(HW_Melanization[Overall_melan], pch=19, cex=2, col="orange")
##### FW
points(FW_Melanization[Overall_melan], pch=19, cex=2, col="blue")

for (i in 1:length(Tot_mel)) {
    text(y=Tot_mel[[i]], x= i ,labels=PA_Results_tot$Family[Overall_melan][[i]],
         adj=c(+0.6,-2), cex=0.7,)
}
```

```
#Draw multiple lines
segments(x0 = 1:100,
         y0 = HW_Melanization[Overall_melan],
         x1 = 1:100,
         y1 = FW_Melanization[Overall_melan])
```

CUSTOMIZED FUNCTIONS

1. RC_lm_listing: generates named copies of the same .txt file of coordinates

```
## INSTRUCTIONS:
# 1)Generate the original landmarks file in the "landmarks folder"
# 3) Run the script with your heart content

RC_lm_listing<- function(ID_position, ID_pattern=".JPG", lm_position){

lmIDlist<- tools::file_path_sans_ext(dir(path = ID_position, pattern = ID_pattern))
                                              # path of the recolored images
LM1 <- tools::file_path_sans_ext(dir(path=lm_position, ".txt"))
                                              #set wd as the landmarks forder
     for (i in 1:length(lmIDlist)) {
        file.copy(from = paste0(lm_position, "/", LM1,".txt"),
                       to = paste0(lm_position,"/",lmIDlist[[i]], ".txt"))
}
library(patternize)
landmarklist<- makeList(lmIDlist, "landmark", prepath = lm_position,  extension =
".txt")
return(landmarkList)
}
```

2. expRC_JPG: Export of recoloured images in JPG

```
# expRC_JPG <- function(rcList, exp_path="") { #rcList is a list
#    wd<- getwd()
#library(recolorize)
#names_imgs<- as.vector(paste0(names(rcList), ".JPG"))
#setwd(exp_path)
#for(i in 1: length(rcList)) {
#           jpeg::writeJPEG(recoloredImage(rcList[[i]]),   target=   paste0("rc_",
names_imgs[i]), quality = 100)
#}
#setwd(wd)
#}
```

3. imgImport: imports images as arrays and list them

```
imgImport <- function(folder="", extension="") {
  library(recolorize)
  imgs_names<-list.files(path=folder, pattern= extension)
## To get the list of file names
                                ## ignore.case=TRUE -> pattern is case insensitive
   listIMGS<-vector("list",length=length(imgs_names)
#NB: remember the final slash in the path
  for (i in 1:length(imgs_names)) {
    listIMGS[[i]]<- readImage(paste0(folder, "/", imgs_names[i]))

  }
  return(listIMGS)
 }
```